**Research Article**

# Automatic urban boundary delineation in equatorial regions using SAR imagery: a comprehensive approach with decomposition, morphology, and statistical active contours

## Fritz Elenda Nkomba[1*], Timothée Kombe[2] and Pierre Ele[3]

Energy, Materials, Modeling & Methods Laboratory (E3M), National Polytechnic School of Douala (NPSD), University of Douala, Cameroons[1]

Technology and Applied Sciences Laboratory (LTSA), Institute University of Technology (IUT), University of Douala, Cameroon[2]

Laboratory of Electrical Engineering, Mechatronic and Signal Treatment, National Advanced School of Engineering, University of Yaoundé I, Cameroon[3]

## Abstract

*In recent years, algorithms have been developed to decompose images into structural and textural components. Radar images, known for all-weather capabilities, prove increasingly valuable in equatorial regions with quasi-permanent cloud cover. As the African population undergoes rapid demographic growth, it becomes imperative to establish automatic mapping methods for radar images. This facilitates timely urban evolution studies within territorial jurisdictions. This paper presented an approach to delineate urban boundaries in synthetic aperture radar (SAR) images from European Remote Sensing Satellite (ERS)-1, focusing on Douala, Cameroon. Our method emphasizes detecting key features, including road networks, urban structures, inhabited areas, and wetlands, considering the unique granularity of SAR imagery. The decomposition technique was applied to road network detection in aerial or satellite imagery. The algorithmic chain employs a combination of textural image analysis and mathematical morphology, utilizing set theory for road network extraction from radar images and aerial photography. Additionally, linear structures are detected through mathematical morphology, followed by the refinement of extracted roads using statistical active contours. Applying wavelet transforms, filtering by rectangularity measure, histogram analysis, Canny contour detection, morphological operators, and watershed transformation demonstrated precise road detection, effectively distinguishing them from other objects. The algorithm proves efficient across urban, rural, and peri-urban contexts. For inhabited areas and wetlands, the algorithm adapts to higher gray levels associated with rooftops and accurately detects extremely low gray levels indicative of water bodies.*

## Keywords

*Linear structures, Watershed lines, Mathematical morphology, Segmentation, Urban area, First order histogram, Wavelet filtering.*

## 1.Introduction

Recent years have been marked by a steady increase in the number of roads and demographic trends. Faced with this reality, many countries and national and international organizations have taken part in an international effort aimed at achieving several key objectives: providing accurate information on the scale of disasters, facilitating the intervention of rescue teams in the event of a major catastrophe, and coordinating international aid to help disaster-stricken regions.

Indeed, in major disaster situations, it becomes extremely difficult for human responders to assess and access the situation on the ground. This is where satellite images come in very handy, as they provide essential information for organizing a rapid and effective response. These images help to orientate rescue teams by providing detailed maps of the damage, and also facilitate the identification of communication routes that are still operational to deliver the necessary aid.

Remote sensing plays an essential role in establishing a rapid and effective response chain to major hazards,

---

*Author for correspondence

enabling authorities to quickly identify areas of interest and assess the situation after a disaster [1, 2]. This has prompted many countries to launch their own satellites and improve the spatial resolution of the sensors on board. However, this improvement has led to an exponential increase in the size of satellite images, from a few kilobytes to gigabytes, making the task of photo-interpreters increasingly difficult. Hence, the growing need for accurate and dependable maps is on the rise, presenting a challenging issue to address.

In the lack of sufficient cartographic resources, those in positions of authority frequently find it difficult to accurately determine the boundaries of urban areas and the borders between neighborhoods [3–5]. This highlights the need to automate damage assessment of linear structures and the identification of passable roads, to save precious time in these critical situations. As a result, the demand and need for reliable maps continues to grow, posing a major challenge.

The extraction of linear structures from very high-resolution satellite imagery is a widely debated topic [3–8]. This can be explained by the radiometric and structural diversity of these sought-after objects in the image [9–13].

Indeed, linear structures present a variable radiometric response from one city or region to another, depending on the type of bituminous cover used in their construction. This variability makes radiometric characterization of these structures particularly complex. In the case of radar images, there are several objects with a similar radiometric response, and the presence of radar noise, known as speckle, makes radiometric characterization of linear structures difficult.

From a geometric perspective, linear structures in satellite images exhibit irregular shapes with local curvatures and occlusions (e.g., bridges, trees, shadows), complicating interpretation. Extracting these structures is intricate due to specific object characteristics. Detecting changes between images taken before and after an event requires multiple processing operations to rectify errors related to varying shots, sensors, and conditions. Ensuring processed images correspond to the same scene is critical. During disasters, existing algorithms face challenges with unprocessed, noisy images, leading to errors in infrastructure damage detection and a high false alarm rate. In such situations, resorting to

traditional visual interpretation becomes necessary, albeit time-consuming. This research aims to identify and extract linear structures, focusing on road networks, settlement boundaries, and wetlands. The method involves multiscale analysis using wavelet filtering and the mathematical watershed approach, followed by filtering based on the object's rectangularity measure and utilizing morphological operators to accentuate outlines and isolate road network axes.

To achieve this objective, the literature on linear structure detection is reviewed in Section 2. Section 3 outlines the methodologies, while Section 4 and covers the study's results and discussion. Section 5 concludes with a brief discussion of the results and prospects.

## 2.Literature review

Remote sensing is both an advanced technology and a scientific discipline that plays an essential role in the observation and analysis of our environment. As a result, it plays a crucial role in defining, monitoring and evaluating natural resource management policies [14]. Thanks to the integration of ground-based measurements and the use of geographic information systems, remote sensing is now making a decisive contribution to solving a range of problems linked to the environment, health, land-use planning, the rational exploitation of natural resources and the prevention of natural disasters [15]. Its potential uses encompass a wide array of domains including agriculture, forestry, hydrology, water resource management, oceanography, geology, cartography, urban development, land surveying, and even business analytics. Nevertheless, the increasing need for accurate maps presents a formidable hurdle [16]. When adequate mapping resources are unavailable, decision-makers frequently encounter obstacles in precisely delineating geographical borders. Therefore, it becomes imperative to create efficient and suitable information technology (IT) solutions. The scrutiny and comprehension of remotely sensed images assume a significant, if not indispensable, role for photo interpreters and subject matter experts during the map production process.

These analytical techniques enable the more straightforward identification of morphological features like road systems and waterway networks. Numerous studies, both contemporary and historical, have addressed the challenge of autonomously detecting road networks in aerial or satellite imagery. These investigations have notably concentrated on

methodologies for detection and road pattern modeling. When it comes to urban analysis, the determination of the urban perimeter is crucial, particularly for assessing the peripheral growth of large cities. Identifying and characterizing urban networks is a crucial step in the urban planning and management process [17]. Nevertheless, this procedure encounters a methodological challenge because urban infrastructures exhibit diversity and are frequently accessible to a limited extent. In developing nations, the identification and description of urban infrastructures (including transportation methods and road surfaces) holds significant relevance [17]. One of the difficulties lies in the fact that, within an urban area, it is not uncommon to change rapidly from a paved road to an unpaved one, which complicates their identification.

In this research, the preference is for the use of mathematical morphology [18–20] to detect urban features from satellite images. This method proves to be the most suitable, focusing on the study of form, particularly for identifying and retrieving linear and planar entities like road systems and off-road skiing paths [21].

The detection of road networks is of particular importance for many remote sensing applications, such as multisource image registration, map updating and automatic navigation [22]. In developing countries, identifying linear configurations holds significant significance. In producing reliable cartographic data [17]. However, the extent of the areas to be mapped and the frequency of updates require the development of efficient algorithmic tools for the detection of map features. we focus on the use of satellite and aerial imagery to detect linear objects, such as the diverse networks within the radar image of Douala (Cameroon), primarily the road and hydrographic systems. While many methods are now available when aiming to automatically or semi-automatically extract road networks from high-resolution images, radar images introduce a unique set of challenges. Traditional methods for detecting linear structures, based on differences in averages between zones, often fail in this case [23].

Multiple approaches have been suggested to extract linear structures from satellite imagery. For example, the Hough transform [24, 25] have been widely used to search for parametric curves (such as line segments or circles) in an image. However, this method can be limited by parametrization restricting the search to line segments. To overcome these challenges, a Markov field-based approach is used to

exploit a priori information on continuity and neighborhood relationships between pixels, enabling the identification of disruptions in continuity within an interferogram [26]. Regrettably, when dealing with satellite images, this technique can only yield fragmented sections of roads. In their article, [27] proposed a method for extracting the road network of Douala city using mathematical morphology and neighborhood processing. However, this approach faced a drawback due to the discontinuity of the structures. Introduced a method based on marked point processes for structure extraction, but it encountered issues of over-detection and omission of linear structures [28]. Another approach by [7]; utilized texture analysis by leveraging spatial connections among pixels. Nonetheless, this technique demanded substantial processing duration and the linear configurations exhibited uneven textures.

An alternative proposed in [12], involved an object-based image classification method that exhibited resilience to noise but encountered difficulties in precisely specifying the desired level of detail [13], utilized the wavelet transform to partition the image into distinct levels of scale, filtering the resulting regions based on rectangularity measures derived from the relationship between the object's boundary length and its enclosed area. Ultimately, they applied morphological operations to sharpen edges and generate a skeleton representing the main axes of the road network.

Given the remarkable achievements of deep learning models in various visual tasks, they have been extensively applied and refined to address road network extraction challenges using remote sensing images. Many of these models have approached road extraction as a semantic object segmentation problem, where roads are treated as distinct objects and separated from the background through semantic segmentation. Proposed a combined approach using a fully convolutional network (FCN) in an ensemble strategy to tackle the imbalance between road and background contents in images [29]. Combated label noise by combining deep neural networks (DNNs) with a noise probabilistic model [30]. In [31], a deep learning model that operates sequentially was utilized to rectify labeling inaccuracies using learned label probability sequences while [32] incorporated conditional dilated convolution modules in a convolutional neural network (CNN) for full-scale feature fusion.

To preserve road segment details, [33] proposed a network architecture that incorporates scale-sensitive modules and scale-fusion modules, designed to adapt to variations in scale. Introduced a network model with a global context-aware design, aimed at harnessing spatial context characteristics and associations to boost the semantic significance of road areas [34]. Delved into the examination of multiscale spatial contextual attributes through the utilization of global spatial feature pyramid pooling [35], while [36] emphasized edge and topology preservation for accurate road contour delineation. [37]; introduced a bidirectional high-resolution network (Bi-HRNet) for predicting node heatmaps and directional connectivity to enhance road segmentation integrity.

To enhance feature representation and predictions, attention mechanisms were incorporated. Introduced position attention, leveraging contextual properties and modules for extracting foreground context information, favoring the inference of occluded areas [38]. Integrated regional attention to focus on foreground contents and suppress road distribution imbalance [39]. Adopted an attention mechanism that operates at a block-level across multiple dimensions, [40, 41] proposed a residual attention scheme for spatially heterogeneous road types.

To address limited annotated samples, [42] used a generative adversarial network (GAN) with weakly supervised segmentation, incorporating image generation and binary image post-processing. [43] added a spatial penalty mechanism to the GAN to balance classes, and [44] employed edge-preserving filtering. Introduced a feature pyramid module and domain adaptation in the GAN, while [45, 46] proposed stage-wise unsupervised domain adaptation. Used a learning strategy that relies on scribbles for weak supervision, employing an encoder-decoder architecture for extracting road segments, which includes the propagation of road labels [47].

For more comprehensive feature encoding, attention mechanisms were combined. Channel and spatial attention modules were parallel or cascaded in certain architectures [48, 49]. Additionally, to address sensor-based property differences, some studies used crowdsourced, multisource, or multimodal data for road extraction [50–52].

This research endeavors to showcase the practicability of retrieving such data from a synthetic aperture radar (SAR) image captured by the European Remote Sensing Satellite (ERS)-1 satellite over urban area of Douala in Cameroon. This locale frequently contends with dense cloudiness, rendering the procurement of images of high optical quality a substantial challenge for a significant portion of the year. In response, we present a detection technique that amalgamates morphological filters (namely, opening, erosion, closing, and dilation), watershed transformation extended predicate logic (EPL) following filtering, and the identification of the original image's contours. Detecting narrower roads (those narrower than the size of a single pixel) presents a significant challenge primarily due to their diminutive dimensions, making the processing application demanding.

## 3.Methods
### 3.1Data utilized and research location
We employed a segment of the SAR image from the ERS-1, which was captured in 2010 at a frequency of 5.3GHz using VV polarization, and had a spatial resolution of 12.5 meters by 12.5 meters.

### 3.2Methods
Currently, numerous studies enable the automatic or semi-automatic detection of road networks on high-resolution optical satellite images. Our approach employs two primary methods: the 2D wavelet transform combined with statistical analysis, as well as the utilization of watersheds and mathematical morphology.
#### 3.2.1Filtering
**Median filter**
To diminish noise within an image, the median filter is a viable option. Noise in an image typically refers to irregular or outlier pixels, such as isolated bright pixels amidst a predominantly dark area, or sporadic pixels scattered throughout the image. The process of image smoothing seeks to alleviate noise by considering neighboring pixels for an average, although this can result in a reduction in image sharpness. The median filter method offers an advantageous alternative in this respect. It reduces noise without compromising image sharpness. This approach is particularly effective when noise is in the form of isolated dots or fine lines. However, it should be noted that this method is only applicable to grayscale images, unlike the smoothing process which can be used on color images.

$G(x,y) = \text{median}\{f(n,m) \mid (n,m) \in S(x,y)\}$ where S is a neighborhood of (x,y)

*Figure 1(a)* displays the European Space Agency (ESA), and *(b)* shows the initial SAR image of Douala.
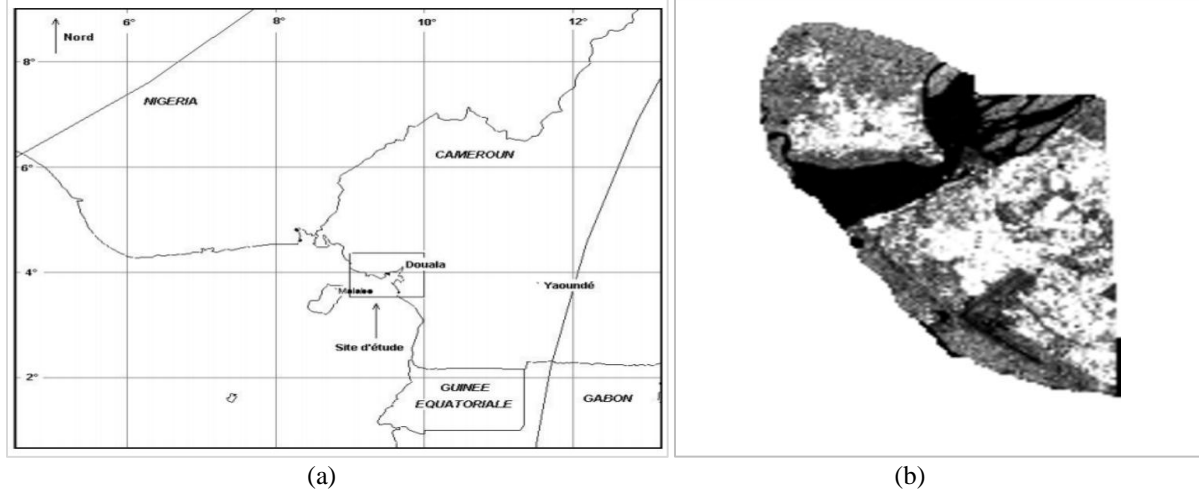
(a)　　　　　　　　　　　　　　　　　(b)

**Figure 1** (a) ESA, (b) Initial SAR image of Douala

**Wavelet filtering**

In general, linear methods are not efficient for signals with singularities. Wavelet methods have been developed for this purpose. A wavelet decomposition of the signal will provide coefficients that represent the signal at different scales and allow to isolate details (including noise). The 2D wavelet bases are usually constructed by tensor products of 1D wavelet bases. Let $\phi$ be the scale function and $\psi$ the wavelet from a 1D multiresolution analysis (MRA) (Equation 1 and 2).

There are two possible constructions:

**Tensor wavelet bases or anisotropic:**

$$\psi_{k,k'}^{j,j'}(x,y) = \psi_{j,k}(x)\psi_{j',k'}(y), j,j'\epsilon\mathbb{Z}, k,k'\epsilon\mathbb{Z} \tag{1}$$

Wavelet from the MRA of $L^2(\mathrm{IR}^2)$: we pose $V_j = V_j \otimes V_j$. The space of details(wavelets) is $W_j$ given by
$V_{j+1} = V_j \oplus W_j$. We have
$V_{j+1} = V_{j+1} \otimes V_{j+1} = (V_j \oplus W_j) \otimes (V_j \oplus W_j)$

So
$W_j$
$= Vect\{\psi_{j,k}(x)\varphi_{j',k'}(y); \varphi_{j,k}(x)\psi_{j',k'}(y); \psi_{j,k}(x)\psi_{j',k'}(y)$
$|\mathrm{k}, \mathrm{k}' \epsilon\mathbb{Z}\} \tag{2}$

For our work, we selected a wavelet from the multi-resolution analysis with an orthogonal wavelet base, coupled with a level 3 Harr wavelet and a mirror filter.

To denoise, we can keep only the wavelet coefficients that correspond to important scales. we threshold the coefficients with a cut-off function which cancels the coefficients inferior to a certain threshold ε, then we reconstruct the signal from the coefficients thus kept. Two types of thresholding can be used, corresponding to two cut-off functions: hard thresholding consists in applying to the coefficients the function (Equation 3).

$$d_\varepsilon : x \mapsto d_\varepsilon(x) := \begin{cases} x & si \ |x| \geq \varepsilon \\ 0 & sinon \end{cases} \tag{3}$$

This function is discontinuous which can cause side effects. We have considered a soft thresholding that uses a continuous function (Equation 4):

$$d_\varepsilon : x \mapsto d_\varepsilon(x) := \begin{cases} x - \varepsilon \ si \ x \geq \varepsilon \\ x + \varepsilon \ si \ x \leq -\varepsilon \\ 0 \qquad sinon \end{cases} \tag{4}$$

Soft thresholding has been employed to mitigate edge effects.

**3.2.2 Analysis of texture using statistical methods of the first order**

Image analysis and manipulation of data rely on two fundamental concepts: texture and structure. Texture refers to a collection of textural elements, which are continuous and repetitive areas where changes are not easily detectable or are detected using available methods. In the context of satellite images, textural elements consist of resolution elements defined by sensor characteristics. These elements share similar luminance values or luminance-derived characteristics (object dimensions) and have spatial relationships. Hence, areas with the same textural value constitute a texture. Here, wavelets from the MRA of $L^2(\mathrm{IR}^2)$ associated with soft thresholding have been used. In *Figure 2*, the multistep image processing approach for urban feature recognition is illustrated, demonstrating the intricate steps involved in the analysis. *Figure 3* provides insight into the

66

"hard" and "soft" thresholding functions, essential components in the processing pipeline. A detailed depiction of the 2D multi-resolution analysis is presented in *Figure 4*, showcasing the method's effectiveness in handling complex urban imagery. *Figure 5* explores into the specifics of the multi-resolution analysis using 2D Harr level wavelet transform, highlighting a key aspect of the methodology employed in the recognition process.
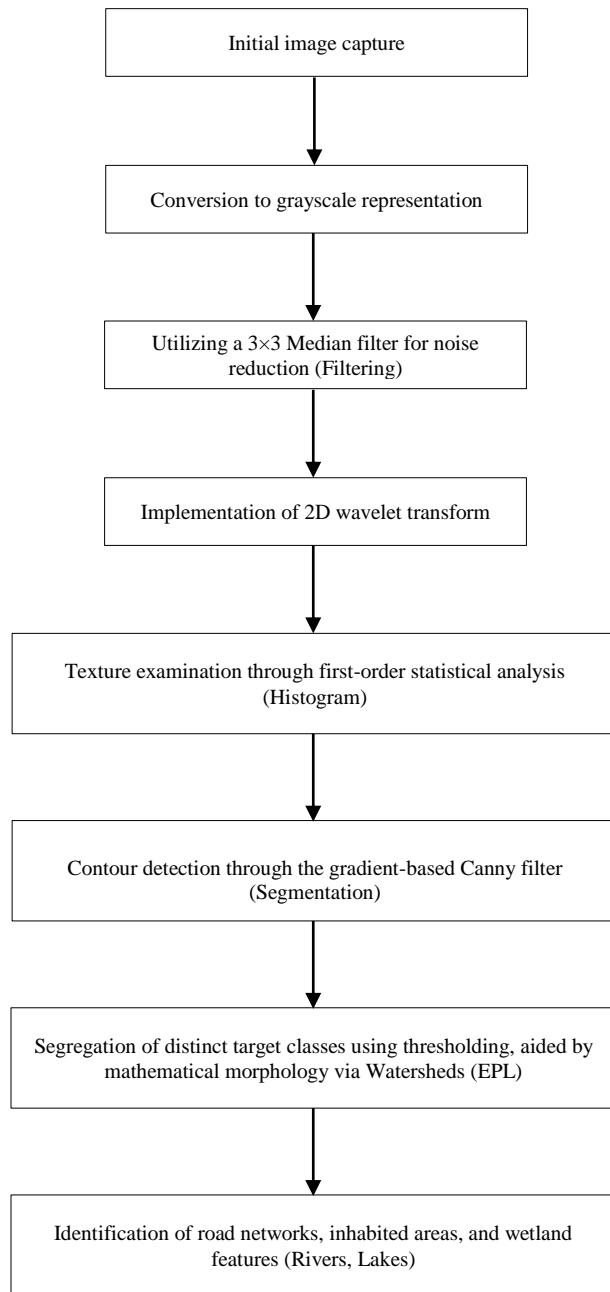


**Figure 3** Hard" and "soft" thresholding functions
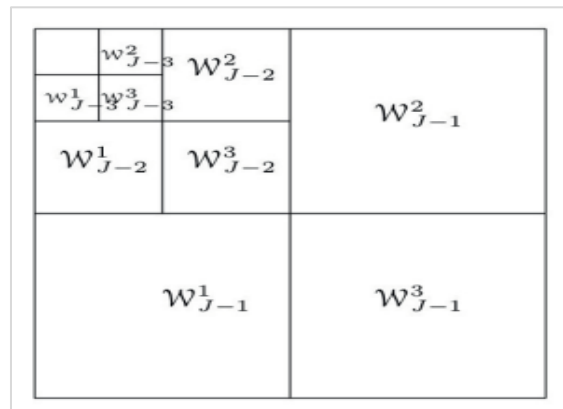


**Figure 4** 2D multi-resolution analysis



Decomposition at level 3
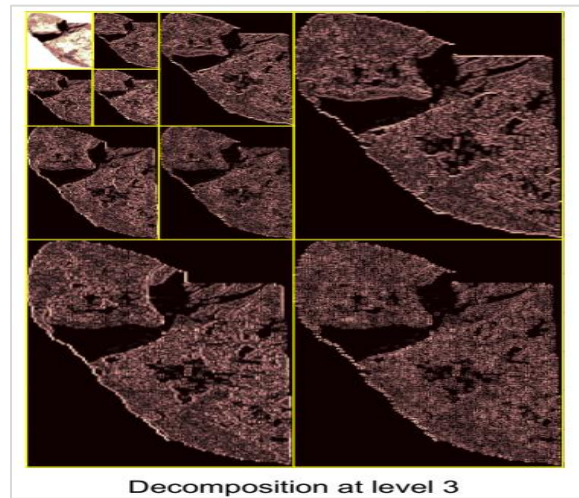
**Figure 5** Multi-resolution analysis 2D Harr level wavelet transform

```
Initial image capture
        ↓
Conversion to grayscale representation
        ↓
Utilizing a 3×3 Median filter for noise
reduction (Filtering)
        ↓
Implementation of 2D wavelet transform
        ↓
Texture examination through first-order statistical analysis
(Histogram)
        ↓
Contour detection through the gradient-based Canny filter
(Segmentation)
        ↓
Segregation of distinct target classes using thresholding, aided by
mathematical morphology via Watersheds (EPL)
        ↓
Identification of road networks, inhabited areas, and wetland
features (Rivers, Lakes)
```

**Figure 2** Multistep image processing for urban feature recognition

Texture analysis involves considering the spatial distribution of gray levels around a pixel in an image. Various texture analysis methods have been developed, with the co-occurrence matrix being a

prominent one. This method computes the probability of gray level pairs (i, j) occurring, given a displacement vector v in a specific direction and orientation. However, it has limitations as it does not consider all pixel directions. An alternative approach proposed in [54] is the texture spectrum method, resembling the co-occurrence matrix approach. It characterizes stochastic properties of gray level distribution but considers all eight neighboring pixels around the target pixel, rather than a single displacement vector. To address these challenges, we adopt a first-order histogram-based analysis method described in [55] as a model for our approach. This

method utilizes histograms to represent the frequency of gray levels within a defined neighborhood. From this histogram, various statistical parameters can be extracted at different levels of complexity. *Figure 6* shows the textural analysis using first-order statistical methods, showcasing the grayscale image and the corresponding histogram of first-order statistics.

It is important to note that the original image must be converted to grayscale before applying median filters, as these filters are specifically designed for grayscale images.
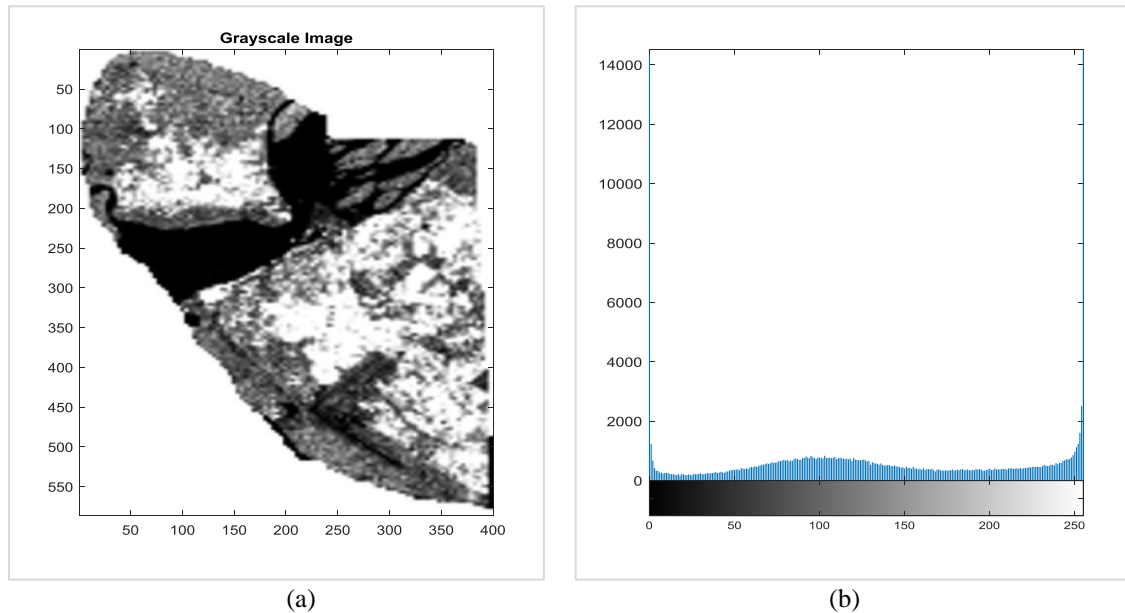


(a)                                                    (b)

**Figure 6** Textural analysis using first-order statistical methods. (a) Image in grayscale. (b) Histogram of first-order statistics

### 3.2.3 Local thresholding by extracting the gradient maxima in one direction (canny filter)

The objective is to keep only the local maxima in one direction of the gradient. The principle is to compare the norm of the gradient at any point M(i,j) of the image with those of its two neighbors M1 and M2 located in the direction of the gradient at a unit distance on either side of M. The moduli of the gradients at M1 and M2 are not known a priori and are interpolated from the gradients computed at two pixels of the image in the vicinity of M1 and M2. The algorithm thus highlights the local maxima in preferred directions (four directions in the proposed example). It then remains to select the maxima to keep using one of the thresholding techniques.

In order to obtain the binary image showing the contours, it is necessary to threshold the image with

the local maxima in the four preferred directions. Indeed, only the most significant local maxima, selected by thresholding, lead to the edge.

### 3.2.4 Mathematical morphology

Mathematical morphology, deeply rooted in set theory, serves as an image analysis technique [21]. It finds its basis in the first law of vision, which posits that any object obscures what lies behind it. In essence, when object A is positioned in front of object B, our visual perception shifts from B to the set-based distinction of B-A. This fundamental concept underscores the inherent opacity of objects in contrast to their translucence, shaping our perspective of them. To articulate this, the mind employs fundamental notions such as inclusion, intersection, union, and more - the foundational principles of morphology - to describe and characterize shapes.

In this context, the objects under examination remain beyond the reach of direct measurement. Consequently, analysts must construct a framework from which measurements can be derived, a process accomplished incrementally through successive transformations that progressively highlight the desired set within the raw image [18]. *Figure 7* shows the Canny gradient filter. This accentuation is achieved through the application of the essential tools of mathematical morphology: Erosion, Dilation, Opening, and Closing. At its core, mathematical morphology hinges on the comparison of objects to be analyzed with a reference object possessing a known form, referred to as the structuring element, which often takes on basic geometrical shapes such as circles, squares, or hexagons (*Figure 8*).
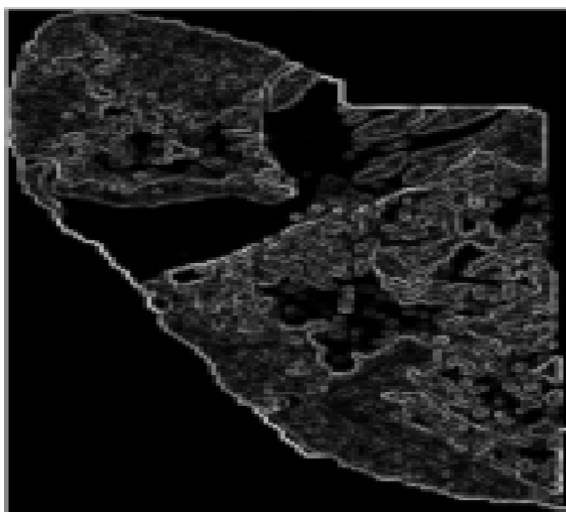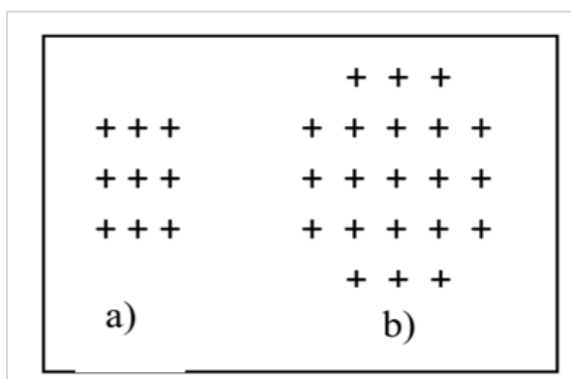


**Figure 7** Canny gradient filter



**Figure 8** Visualization of a structuring element: (a) square and (b) hexagonal

**Transformation by erosion**

Consider a space $IR^2$ partially occupied by a set X and a structuring element Bx. Bx is then moved so that its center occupies.

The erosion principle applied to a 10×4 binary image (*Figure 9*) using a 3×3 unitary square structuring element (*Figure 10*) with 8th order connectedness is illustrated in *Figure 11*. This involves placing the central pixel of the structuring element on each pixel of the image. If the logical product of all points in the structuring element with those in the image results in 1, we assign the value 1 to the centered pixel. If any logical product yields 0, we assign 0 to the corresponding centered pixel. The outcome is specific to replacing voids with 0s for managing the image edges, consistent throughout subsequent processing. Note that a symmetrical edge management approach would yield different results, although this aspect is not discussed here. For grayscale images, binarization is crucial, ensuring only two values, 0 and 1, representing dark and light parts, respectively [17]. Thresholding is employed, assigning 0 to levels between the minimum threshold (S1) and maximum threshold (S2), while levels below S1 and above S2 are assigned the value 1. The choice of thresholding levels depends on the information sought.

Successively all the positions x of the space. For each position, we ask the following question: is Bx completely included in X? In other words: is Bx ⊂ X? The set of positions x corresponding to a positive answer forms a new set Y called eroded from X by Bx. This set satisfies the Equation 5.

$$Y = \{X : B_X(x) \subset X\} \ We \ note \ Y = E^B(X) \quad (5)$$

**Transformation by Dilatation**

In the case of a Dilatation, for each position of the structuring element $B_x$ in the set X, we ask the question: does $B_x$ touch X? in other words: $B_x \cap X \neq 0$? The set of points in IR2 corresponding to positive answers forms a new set Y called the Eroded of X. The dilation transformation is written as shown in Equation 6.

$$Y = D^B(X) \quad (6)$$

The Erosion of the dilated image of *Figure 10* gives the results presented in *Figure 12*. All the edges of the image become dark.

The principle consists in positioning the central pixel of the structuring element on each pixel of the image. If the logical sum of all the pixels of the structuring element with those of the image is different from 0 at least at one point, we assign the value 1 to the

centered pixel. If the logical sum is 0 at all points, we assign the value 0 to the corresponding centered pixel *(Figure 13)*. The result of the dilation of the image of *Figure 9* is given in *Figure 14*. We thus obtain a unitary image. The Erosion and the Dilatation being iterative transformations, and to improve the results sought, one sometimes applies a transformation by Dilatation on an eroded or an Erosion on a dilated. These two types of transformations are called respectively, Closing and Opening, that is to say:

Diltation + Erosion → Closing;

Erosion + Dilatation → Opening;

**Opening**

If we expand by its transpose each point x of EB (X), it will be replaced by its structuring element Bx. The transformed set $D^B(E^B(X))$ will correspond to the union of all these elements Bx, such that $x \in E^B(X)$. We can also say that, the closure is the space that is not swept when the structuring element is fully included in the complement of the set. The opening is expressed as $O^B$ (X), or $X^B$ and is defined as Equation 7.

$$O^B (= D^B(E^B(X)) \qquad (7)$$

The Dilatation of the eroded image in *Figure 8* gives the results shown in *Figure 11*. We observe an enrichment in bright areas.

**Closing**

The process of dilating a set X with a structuring element Bx, followed by an Erosion by the same structuring element, corresponds to a closing operation. It is expressed by $F^B$ (X) or $X^B$. It is defeated by Equation 8.

$$F^B(X^C) = (O^B(X))^C \qquad (8)$$

*Figure 15* illustrates the opening of the image in *Figure 6* using a 3×3 unitary structuring element, while *Figure 16* depicts the closing of the image in *Figure 6* with a unitary 3×3 structuring element. *Figure 17* shows the opening-closing of the thresholded reconstruction barrier



**Figure 9** Initial shape of a 10×4 binary image



**Figure 10** Square 3×3 structural element



**Figure 11** Example illustrating the Erosion transformation for three positions of the 3×3 square structuring element



**Figure 12** Eroded shape of the 10×4 binary image in Figure 10



**Figure 13** Example illustrating the expansion transformation for three positions of the 3×3 square structuring element

| 1 | 1 | 1 | 1 | 1 | 1 | 1 | 1 | 1 | 1 |
|---|---|---|---|---|---|---|---|---|---|
| 1 | 1 | 1 | 1 | 1 | 1 | 1 | 1 | 1 | 1 |
| 1 | 1 | 1 | 1 | 1 | 1 | 1 | 1 | 1 | 1 |
| 1 | 1 | 1 | 1 | 1 | 1 | 1 | 1 | 1 | 1 |

**Figure 14** Dilatation of the image of figure 5 by a unitary 3×3 structuring element

| 1 | 1 | 1 | 1 | 0 | 0 | 1 | 1 | 1 | 1 |
|---|---|---|---|---|---|---|---|---|---|
| 1 | 1 | 1 | 1 | 0 | 0 | 1 | 1 | 1 | 1 |
| 1 | 1 | 1 | 1 | 0 | 0 | 1 | 1 | 1 | 1 |
| 1 | 1 | 1 | 1 | 0 | 0 | 1 | 1 | 1 | 1 |

**Figure 15** Opening of the image in figure 6 by a 3×3 unitary structuring element

| 0 | 0 | 0 | 0 | 0 | 0 | 0 | 0 | 0 | 0 |
|---|---|---|---|---|---|---|---|---|---|
| 0 | 1 | 1 | 1 | 1 | 1 | 1 | 1 | 1 | 0 |
| 0 | 1 | 1 | 1 | 1 | 1 | 1 | 1 | 1 | 0 |
| 0 | 0 | 0 | 0 | 0 | 0 | 0 | 0 | 0 | 0 |

**Figure 16** Closing of the image of figure 6 by a unitary 3×3 structuring element



**Figure 17** Opening-closing of the thresholded reconstruction barrier

### 3.3 Extraction of linear structure

The procedure for extracting linear structures is outlined in *Figure 2,* encompassing both aerial photographs and radar images. When dealing with aerial photographs, a critical step involves the conversion of the image into grayscale to facilitate subsequent filtering operations. The integration of the wavelet transforms guides the determination of an appropriate scale, thereby mitigating the risks of excessive or inadequate segmentation. A refinement stage follows, employing a Median filter to enhance the quality of the grayscale image.

Subsequently, the filtered image undergoes an in-depth analysis through first-order statistical techniques, contributing to a comprehensive understanding of its texture. Concomitantly, the application of the Canny filter engages in edge detection. The synergy between morphological operators and segmentation through the Watershed method, executed in accordance with a specified threshold, effectively demarcates distinct classes necessitated for detection purposes.

### 3.3.1 Methodology

Our methodological approach encompasses a multi-step extraction process, wherein pivotal stages encompass textural analysis and filtering. The employment of morphological operators, including Erosion, Dilation, Closing, and Opening, serves to accentuate the distinct land use patterns. A subsequent refinement is achieved through the application of Watershed segmentation EPL, further enhancing the precision of the targeted outcome, which in this case is the layout of road networks.

This complementary strategy effectively tackles challenges such as discontinuities, over-detection, and omissions that are commonly encountered when utilizing automatic methods relying on textural analysis through mathematical morphology for the extraction of linear structures. The images utilized in our study were obtained from SAR images captured by the ERS1 satellite of the ESA. Due to the unavailability of more recent image data, our theoretical framework was applied to an image depicting the Douala region in Cameroon, which was captured on August 23, 2010. To streamline computations and underscore the relevance of our chosen methodology, we concentrated on a specific section of the image measuring 640×400 pixels. Only on-the-fly parameters were employed. For reference, the characteristics of the image are summarized in *Table 1*.

In a second application, we focused our efforts on an aerial photograph depicting the topography of Douala city in Cameroon. Utilizing a dedicated algorithm within the MATLAB software environment, we successfully extracted linear structures from these images.

### 3.3.2 Watersheds

The Watershed method, as outlined in references [56] and [57], stands as a fundamental approach in mathematical morphology for image segmentation. This technique utilizes a geographical representation to depict images, where an image is described by a numerical function. This conceptualization envisions the image as a topographic relief, where the gray level of each point is analogous to an altitude value.

Central to the Watershed method is the concept of EPL, closely intertwined with the notion of regional minima. The process often involves a flooding operation, also known as immersion. In this visualization, the image is likened to a topographical landscape, where clear structures represent peaks and dark structures depict valleys. Envision this metaphorical terrain being punctured at the sites of minima. Subsequently, the topographic surface gradually becomes immersed in a vast body of water, often considered infinitely expansive for experimental ease. As the water flows through these perforations (local minima), the water level rises at a constant pace, creating a uniform water level across all catchment areas. It's crucial to emphasize that water can only enter valleys through their respective minima.

Upon the convergence of waters originating from different minima, barriers or dams naturally form to prevent their intermingling. As the complete topographic surface becomes submerged, only the raised barriers or embankments remain visible, effectively delineating watershed areas. The count of these emergent dikes is determined by the number of local minima in the function. At the culmination of the immersion process, the collective set of embankments forms closed contours, referred to as Watershed Lines, as depicted in *Figure 18* [58].
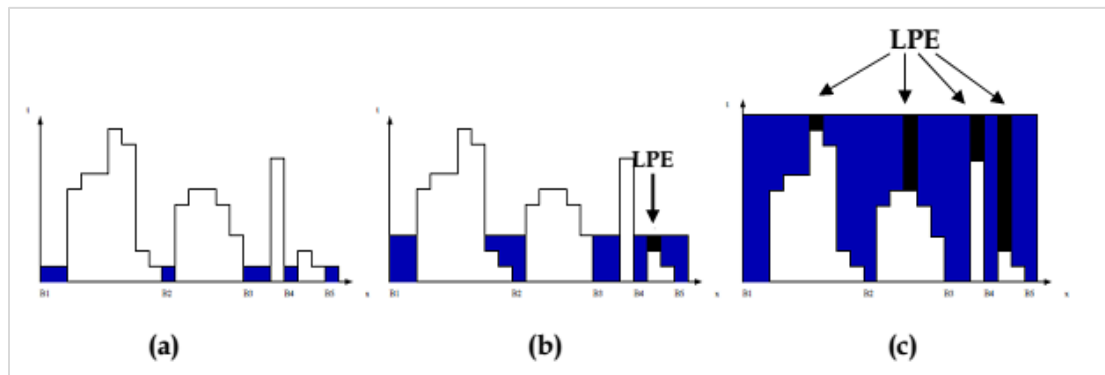


**Figure 18** Construction process of EPL or LPE: (a) Immersion of the relief from its minima. (b) Creation of a barrier when two watersheds intersect (c) Completed watershed map [58]

Unfortunately, due to prevalent noise in real-world images, the EPL algorithm is applied within the context of the gradient image of the intended segmentation image. This strategic choice is motivated by the gradient's ability to distinguish between areas of homogeneity and heterogeneity. Pixels in heterogeneous regions exhibit more pronounced gradients, indicating significant changes in elevation.

As a result, homogeneous image areas correspond to regional minima within the gradient image. In this context, the EPL essentially corresponds to the peaks within the gradient image, mirroring the contours of the original image. However, this approach leads to a significant problem of over-segmentation, as illustrated in *Figure 3*.

To address this issue, a crucial measure involves ensuring that only one gradient minimum is present within each region earmarked for segmentation. This requirement aligns with the concept of flooding the topographic surface formed by the image's gradient, not from its native minima but from designated markers known as 'M markers' [59]. This variant of EPL is commonly referred to as marker-controlled EPL.

The fundamental idea behind homotopy modification of the gradient is to establish markers for intended segmentation regions as the minima of the gradient,

while systematically eliminating all other undesirable minima. Following this process, the modified gradient is inundated with the designated markers. As a result, a singular and distinct EPL emerges between every pair of markers, naturally aligning itself with the contours of the objects already pre-detected through gradient analysis. *Figure 19* presents the Watershed segmentation image and the extracted road network from the original 640×400 image of Douala city.

To derive the gradient image, a morphological gradient is computed for each individual spectral band present in the image [60−62]. The morphological gradient's definition is encapsulated by the relationship Equation 9.

$$G(A) = \delta B(A) - \varepsilon B(A) \qquad (9)$$

Here, δB and εB signify dilation and erosion operators respectively, both applied using a 3×3 square-shaped structuring elements denoted as 'B', while 'A' denotes the image itself. The ultimate elevation image is synthesized by amalgamating elevation values from distinct spectral bands through the utilization of the Euclidean norm.

If the gradient associated with the 'i' the spectral band is represented by Gi, and 'NB' signifies the total number of bands, the final gradient is defined through the subsequent Equation 10.

$$G = \sqrt{\sum_{i=0}^{N_B} G_i^{\,2}} \qquad (10)$$



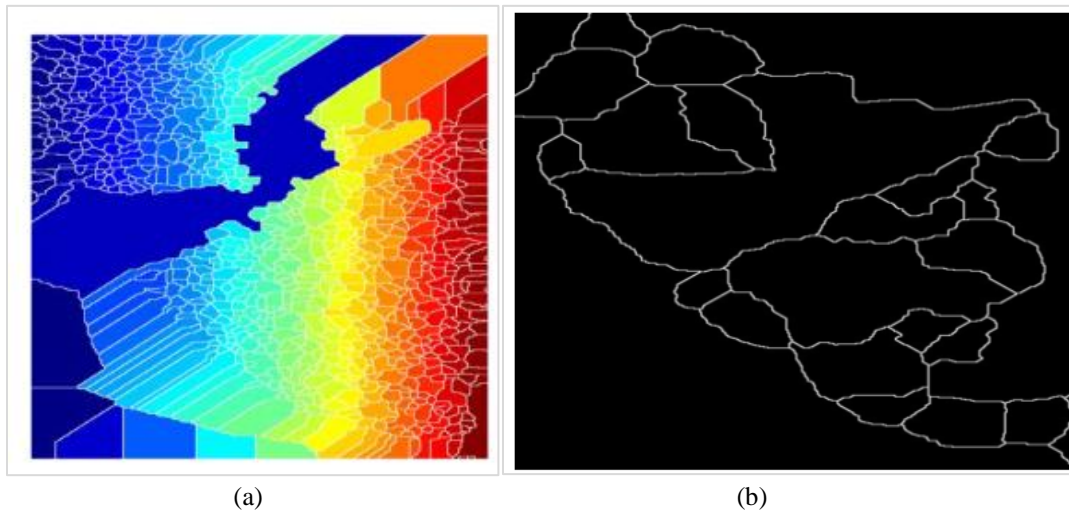(a)                                    (b)

**Figure 19** a) Watershed segmentation image of the original 640×400 image of Douala city b) Road network extracted from the original 640×400 image of Douala city

## 4.Results
### 4.1Image processing and detection of road networks

*Figures 20(a), 21(a), 22(a),* and *23(a)* depict four median-filtered grayscale images, extracted from various sources— the first from a satellite image of Douala city in Cameroon, the second from an aerial photograph of Cross's Douala field, and the third and fourth from aerial photographs of Libreville city in Gabon. These images represent densely populated urban areas with some minor artifacts, including noise, cars on road surfaces, buildings, and tree shadows.

In *Figures 20(b), 21(b), 22(b),* and *23(b),* the results of applying the wavelet transform (2D Harr level 3) for image segmentation at different scale levels are illustrated. Subsequently, the segmented regions are filtered based on their rectangularity measure, determined by the ratio of an object's perimeter to its surface.

*Figures 20(c), 21(c), 22(c)*, and *23(c)* display the first-order histograms of the images obtained after the wavelet transform. Following this, the Canny contour detector is applied.

*Figures 20(d), 21(d), 22(d),* and *23(d)* demonstrate the results obtained by applying morphological open-closed operators through thresholded reconstruction. *Figures 20(e), 21(e), 22(e),* and *23(e)* showcase the results obtained following the application of the watershed method.

In *Figures 20(f), 21(f), 22(f),* and *23(f),* it is evident that the main road axes in the test images were accurately detected. The multiscale analysis facilitated the distinction between road contours and those belonging to other objects such as buildings, while also eliminating contours that describe small objects. These results highlight the accuracy and efficiency of our algorithm in road identification across urban, rural, and peri-urban contexts.

## 4.2 Detection of inhabited area and wetlands

The same algorithm was applied with a few adjustments, incorporating considerations for the detection of populated areas characterized by significantly higher gray levels due to the presence of rooftops made of highly reflective materials. This aspect was integrated into the histogram analysis. Furthermore, the identification of wetland areas, distinguished by their extremely low gray levels representing water bodies, was addressed.
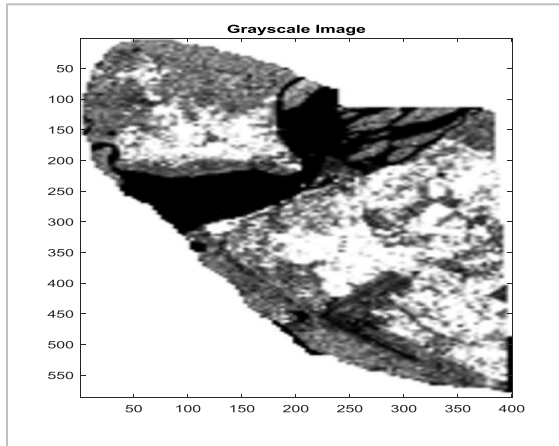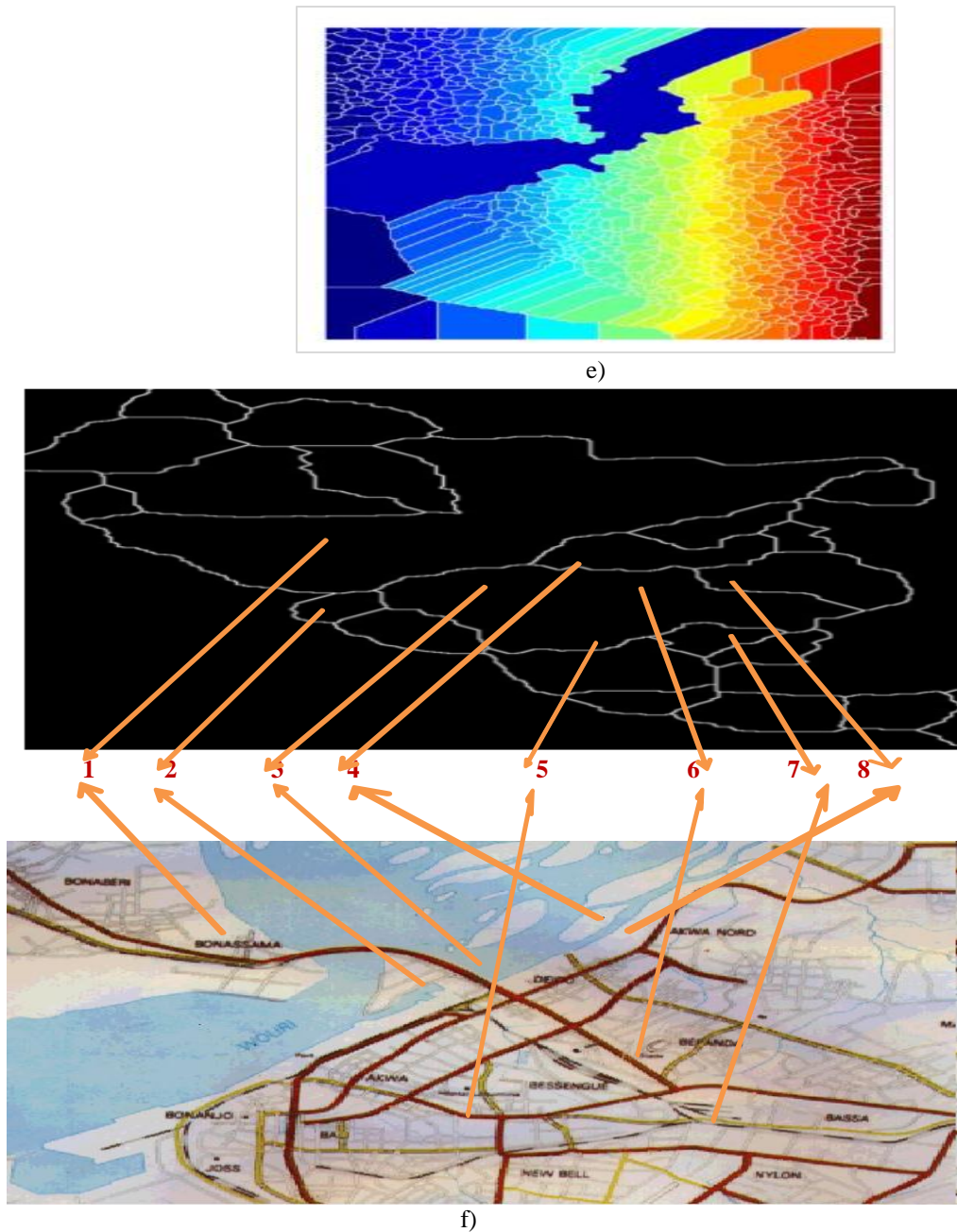
a)
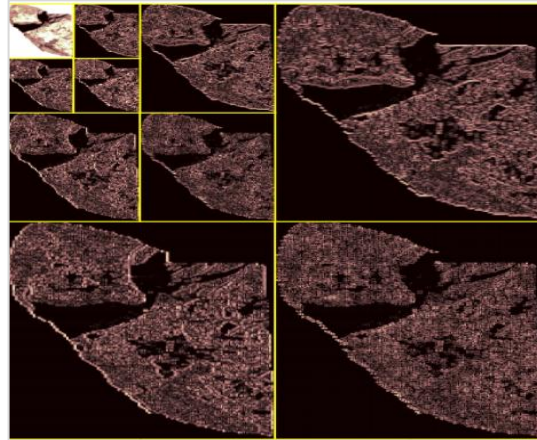
b)
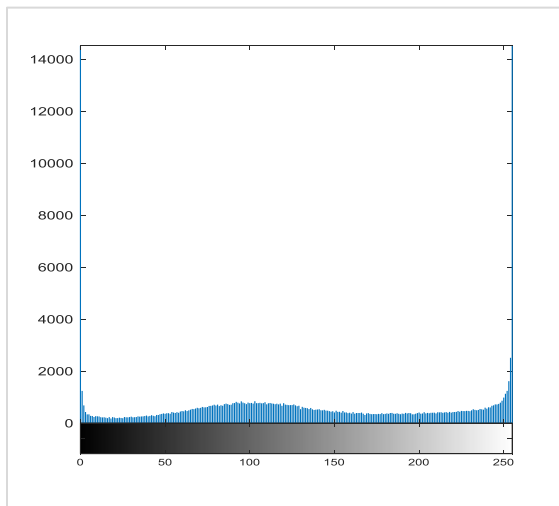
c)

d)

Figure 20 a) Grayscale image filtered by the median filter, b) wavelet transform, c) histogram d) thresholded reconstruction after opening-closing, e) LPE, f) road system (1, 2, 3, 4, 5)
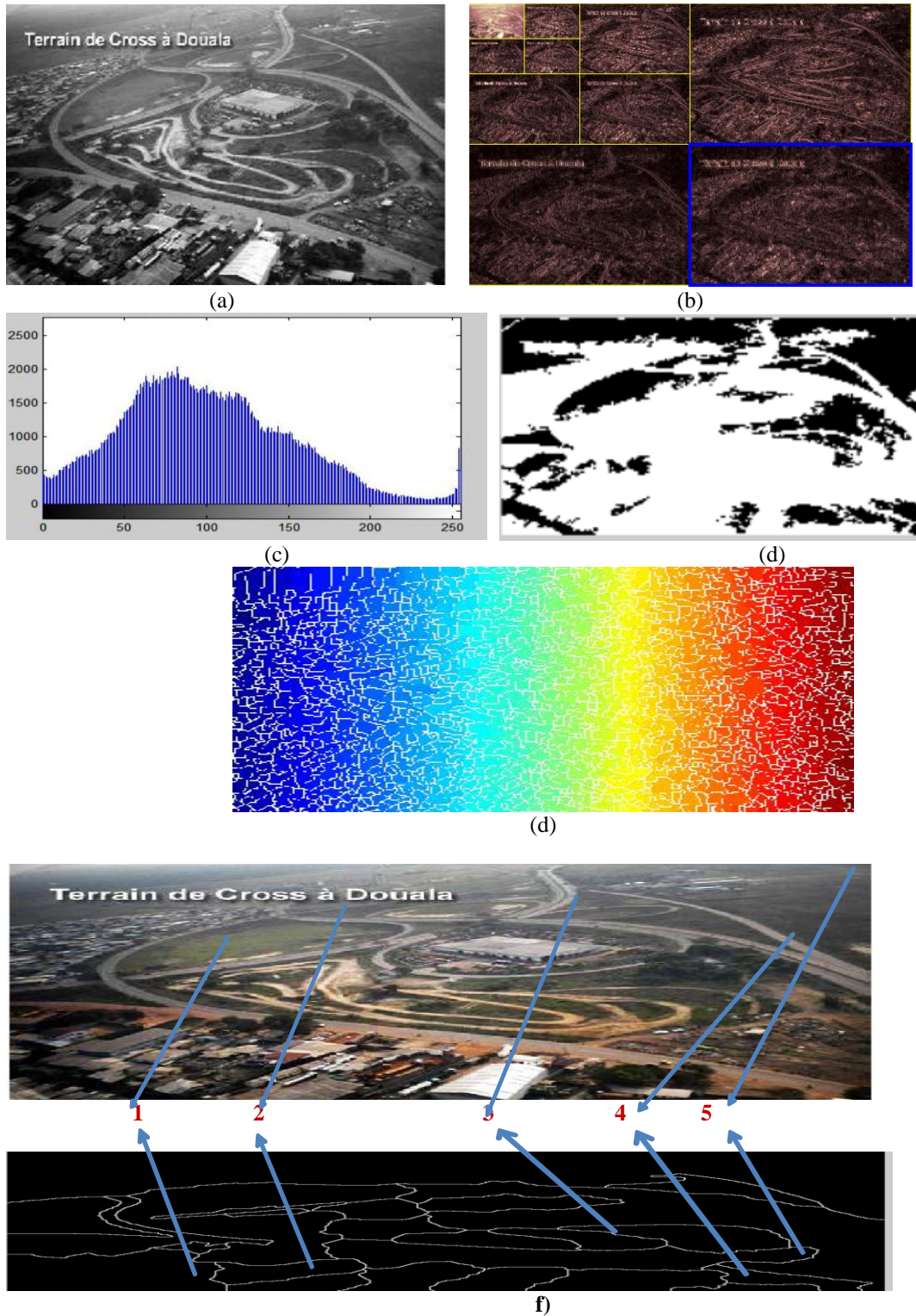
(a)



(b)



(c)



(d)



(d)



f)

**Figure 21** a) Grayscale image filtered by the median filter, b) wavelet transform, c) histogram d) thresholded reconstruction after opening-closing, e) LPE, f) road system

Figure 22 a) Grayscale image filtered by the median filter, b) wavelet transform, c) histogram d) thresholded reconstruction after opening-closing, e) LPE, f) road system

(a)

(b)

(c)

(d)

(e)

(f)

**Figure 23** a) grayscale image filtered by the median filter, b) wavelet transform, c) histogram d) thresholded reconstruction after opening-closing, e) LPE, f) road system
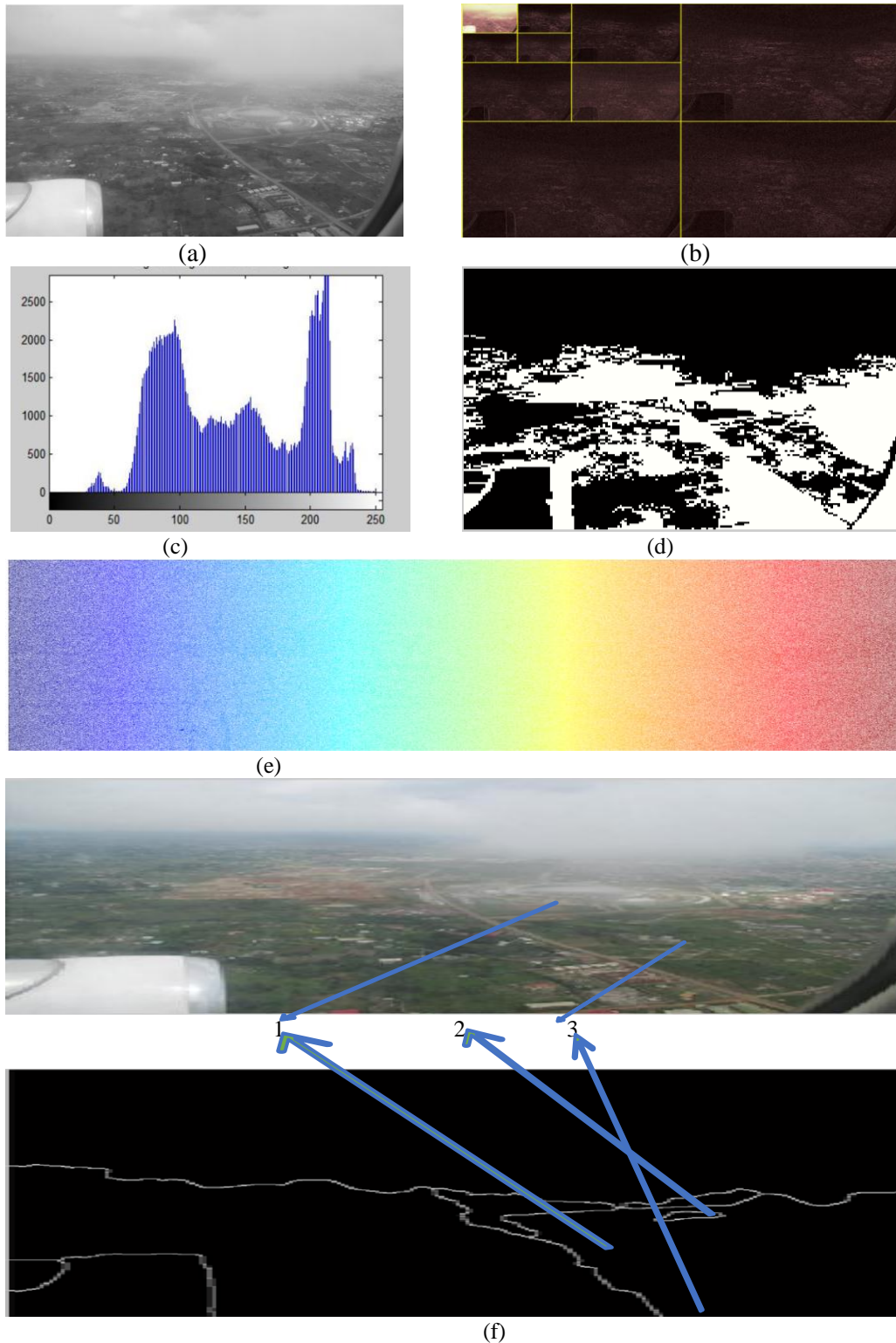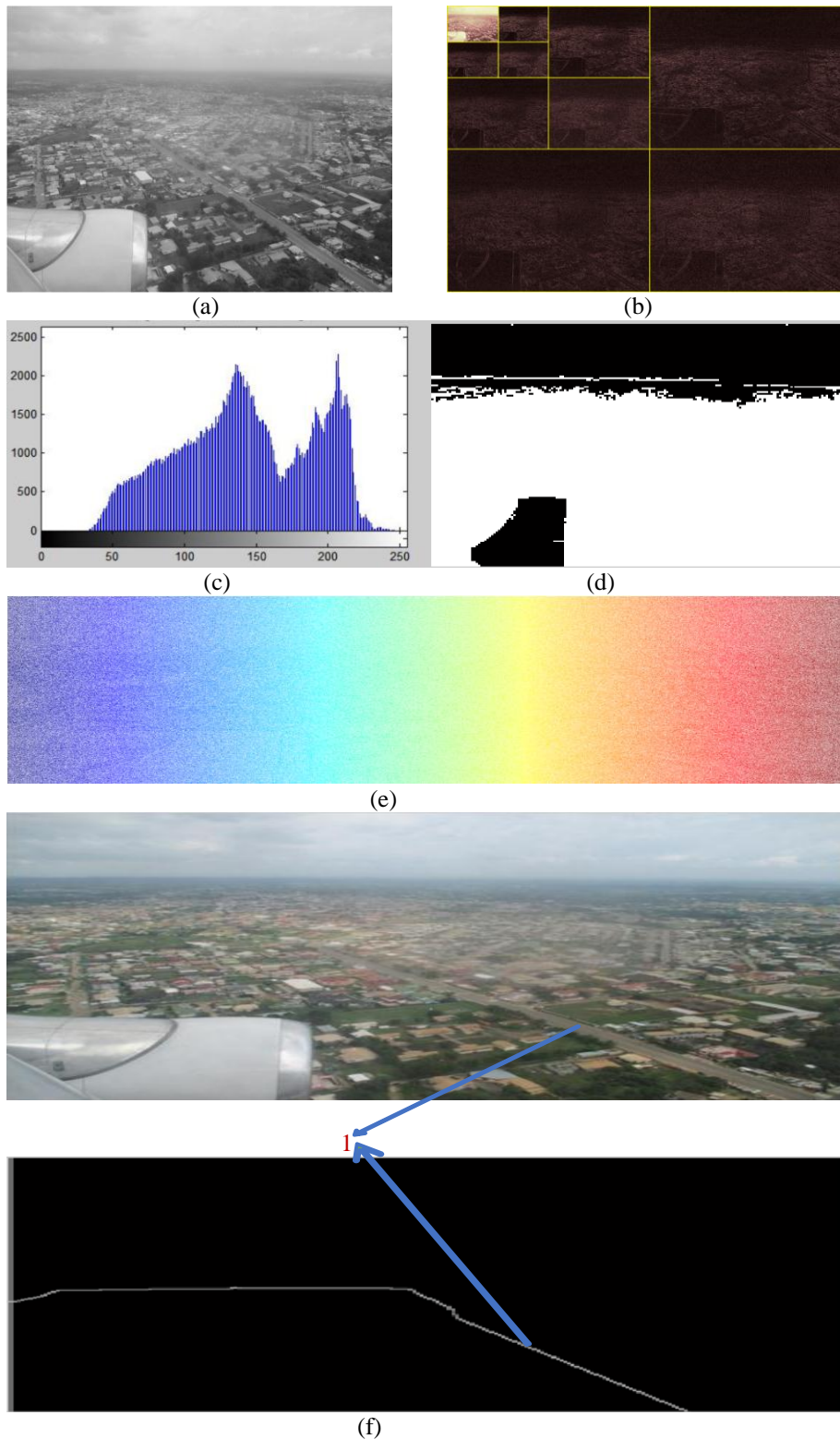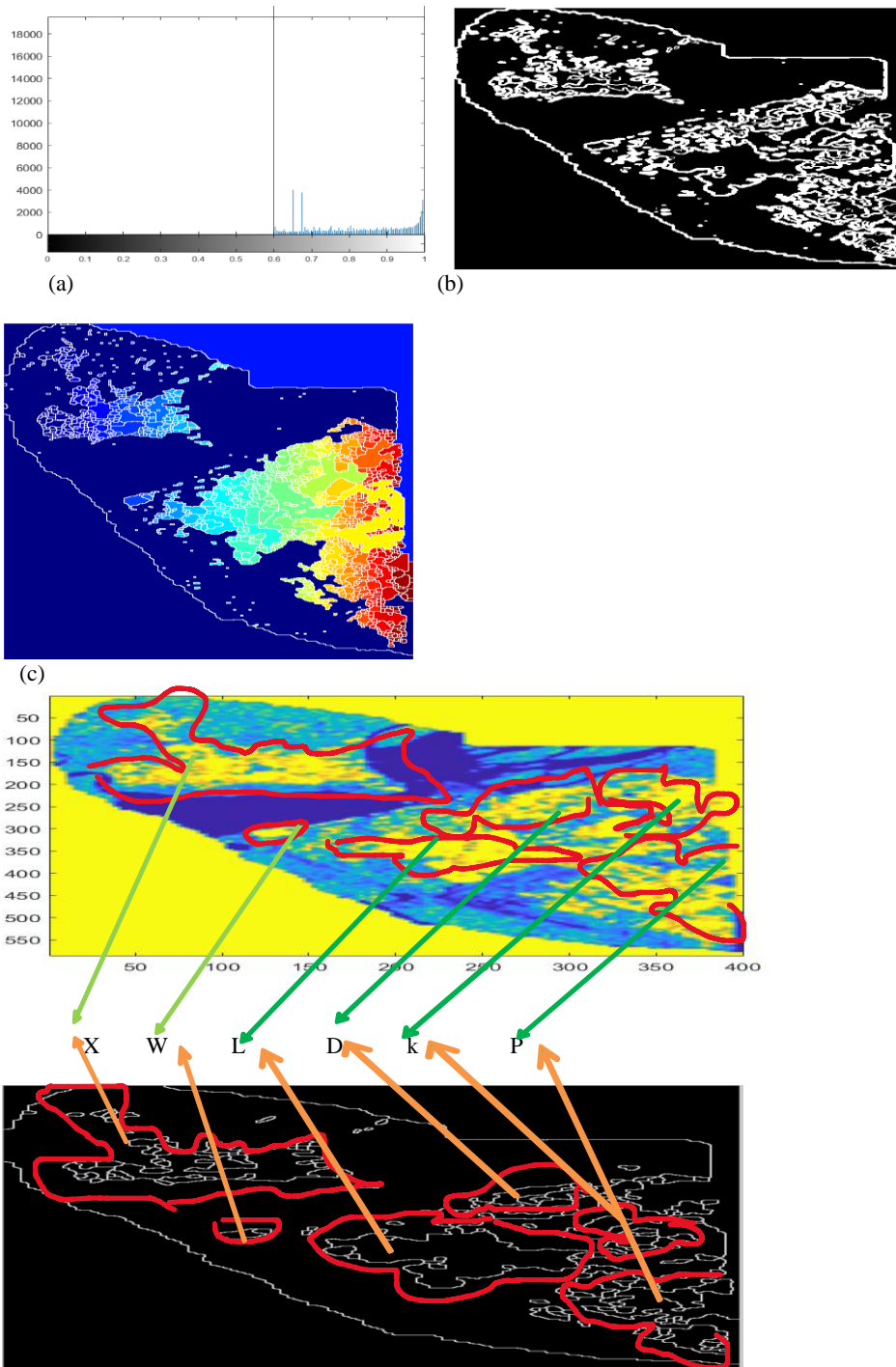
(a)

(b)

(c)

**Figure 24** a) Histogram Analysis b) thresholded reconstruction using opening-closing c) Watershed transformation (EPL), d) populated area
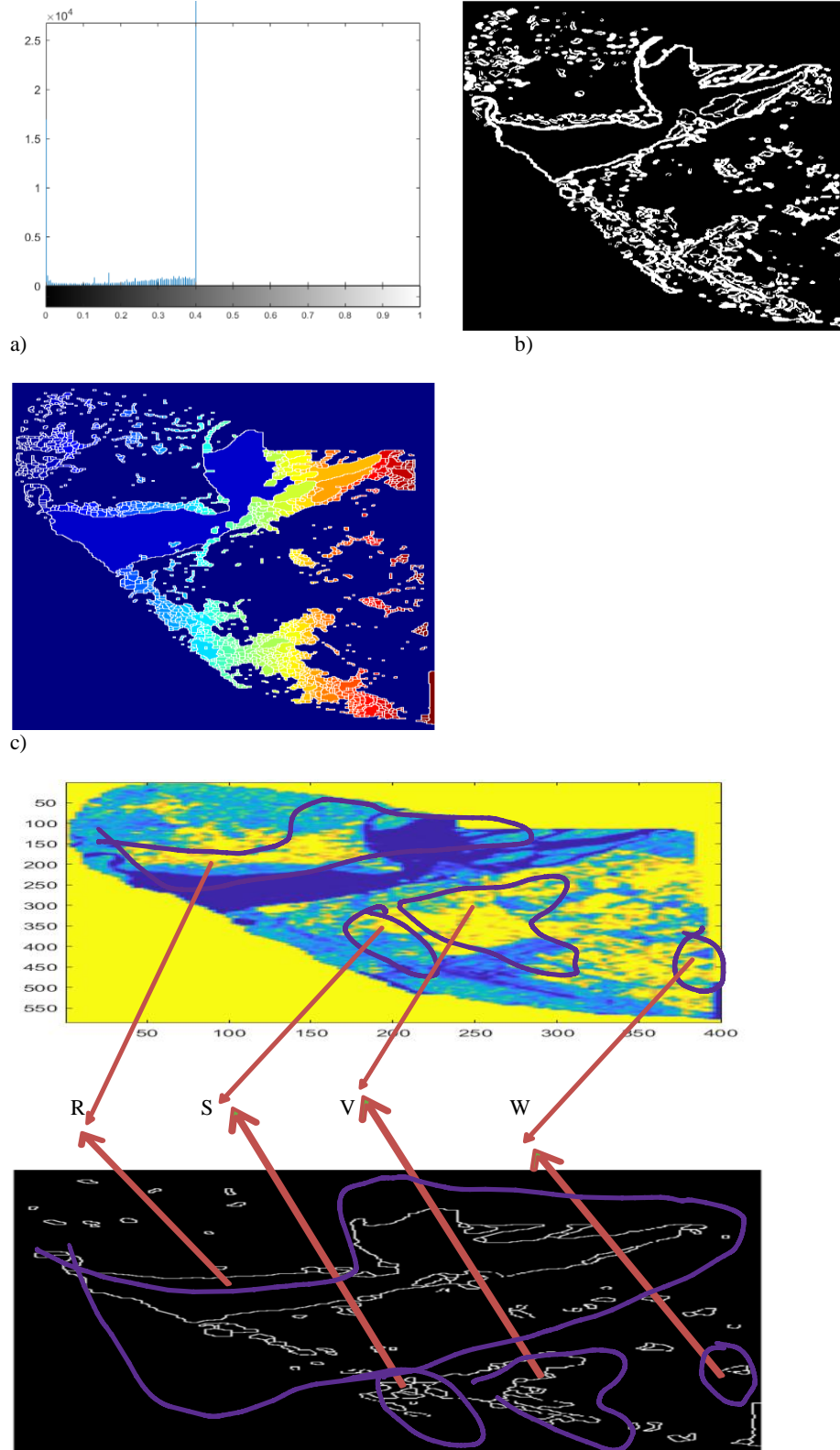
a)

b)



c)



R   S   V   W

**Figure 25**: a) Histogram analysis, b) Application of opening-closing thresholded reconstruction, c) Watershed transformation (LPE), d) swampy area

# 5.Discussion
## 5.1Interpretation of the finding
The landscape of linear structure detection methods was broadly categorized into two main approaches: local and global extraction methodologies. These strategies encompassed a wide range of techniques aimed at identifying linear structures, often treating them as invariant entities regardless of the scale of observation. However, within the realm of signal and image processing, scale held paramount significance, governing the perception and characterization of features, particularly in image analysis.

The linear structure detection algorithm commenced with the conversion of the input image to grayscale. This preliminary step was pivotal to striking a balance between over-segmentation and under-segmentation tendencies. Subsequently, the application of the Median filter performed noise reduction, entailing a simple smoothing of the image and effectively mitigating the influence of outlier pixels through their averaging with neighboring pixels. However, while noise reduction was achieved, the trade-off was a reduction in image sharpness.

The utility of the Median filter became pronounced when noise was manifested as isolated points or fine lines. Yet, it's important to note its limitation: it's only applicable to grayscale images. To address a broader range of noise patterns, the wavelet transform was employed. Subsequently, the Canny filter calculated the intensity gradient of each pixel, revealing the direction of the most pronounced change in intensity, from light to dark, and the corresponding rate of change.

This enabled the delineation of object edges across the study area. A subsequent assessment of edge detection was executed through the Watershed method. Here, the gradient image of the image to be segmented underwent scrutiny. Homogeneous regions of the original image emerged as regional minima within the gradient image. The resultant EPL aligned itself with the peaks in the gradient image, essentially tracing the contours of the initial image.

To avert the issue of over-segmentation, the condition was established that only a single gradient minimum should emerge within each segmentable region. This equated to flooding the image's gradient-defined topographic surface not from its native minima, but rather from designated markers. The application of morphological operators, specifically Opening and Closing, contributed to the elimination of peninsulas and the identification of regional maxima within the image.

This iterative process superimposed regional maxima on the original image, followed by a repeated sequence of Opening and Closing operations. This dynamic iteration facilitated the detection of distinct regions within the image, separated using the EPL. The utilization of thresholded reconstruction opening-Closing aided in discarding extraneous features while preserving vital contours.

The outcomes of this linear structure detection process, as depicted in *Figures 19f* and *20f*, showcased the influence of various thresholds. A comparison with the road network map of Douala city (*Figure 19f*) revealed that not all roads were successfully detected. This could be attributed to several factors, including roads narrower than a single pixel and road segments obscured by the roofs of metal-sheeted houses, which exhibited high radiometric levels.

The algorithm employed for road network detection was then extended to a SAR image of the Douala region in Cameroon. This expanded application involved the detection of specific features like settlements and wetlands, taking into account the intensity variations following diverse filtering. The resulting images are presented in *Figures 24(d)* and *25(d)*.

## Comparison to other studies
Numerous researchers have endeavored to categorize linear structure extraction methods, often opting for a classification into two main groups: automatic and semi-automatic methods. The former encompasses route extraction approaches, including unsupervised segmentation and classification, Markov fields on graphs, and interpretation systems. The latter consists of tracking and filtering methods, active edge, and dynamic programming.

In our analysis of linear structure extraction techniques, we adopted the classification of local methods and global methods, considering them to be the most suitable. These approaches follow a logic commonly employed in image processing, analyzing information at both pixel and object levels. Additionally, we introduced a third category comprising multiscale techniques that connect local information to global information, aiming to identify the optimal scale for analyzing the object of interest.

Fritz Elenda Nkomba et al.

The watershed method is also included in this third category.

**Table 1 Comparison of different algorithms**

| Reference | Category | method | Satellite | resolution | Advantages | Disadvantages |
|---|---|---|---|---|---|---|
| Mohammadzadeh et al. [3] | local | mathematical morphology | IKONOS | high | ✓Rectangular or square-shaped structures are suitable for the enhancement of linear elements | ✓Requires user intervention |
| Chaudhuri et al. [4] | local | Mathematical morphology | IKONOS | high | | ✓Linear features lack consistent textures |
| Jinxin et al [5] Sun and Mao [6] | local | edge | Quickbird RADARSAT- | high | ✓ The parallel edges of linear structures provide vital information | ✓Confusion between road contours and those of other objects (buildings, rivers) |
| Mena and Malpica [7] | local | texture | - | high | ✓ Exploits spatial relationships between pixels) | ✓Considerable time calculation ✓ Linear features lack consistent textures |
| Zhang and Lin [8] Zhu et al. [9] | local | Classification pixels | Aérienne RADARSAT-2 | very high | ✓ Easy to apply | ✓ Noise-sensitive |
| Herumurti et al. [10] Wei and Feng [11] | global | Hough transform | - | high | ✓ Easy to apply ✓ Noise-resistant | ✓ High error rate errors ✓Unable to extract curves |
| Shackelford and Davis [12] | global | Object classification | IKONOS | high | ✓ Noise-resistant | ✓Difficult to define the level of detail desired |
| Naouai et al. [13] | multiscale analysis | Wavelets transform | Quickbird | high | ✓ Determines the correct scale for route identification | ✓Difficult to implement |
| Zhang et al. [29] | Global | Ensemble Spatial Consistency Fully Convolutional Network (ESC-FCN) for Imbalanced Aerial Road Extraction | | high | Imbalance Handling Ensemble Strategy Effective Semantic Segmentation | ✓Computational Complexity ✓Dataset Dependency |
| Li et al. [30] | local | Robust Deep Neural Network (RDNN) for Road Extraction from Remote Sensing Images with Noisy Labels | | high | ✓Noise Probabilistic Model ✓True Label Predictor (TLP) ✓Noise Label Estimator (NLE) ✓Regularization ✓Experimental Validation | ✓Complexity ✓Model Complexity ✓Hyperparameter Tuning ✓Applicability |
| Li et al. [31] | Local | Sequence Deep Learning (SDL) Framework for Robust Road | | high | -Label Noise Correction -Utilization of Label Probability | ✓Complexity ✓Computational Resources |

| Reference | Category | method | Satellite | resolution | Advantages | Disadvantages |
|---|---|---|---|---|---|---|
| | | Extraction | | | Sequence -Adaptive Label Correction -Noise Correction Loss Function | |
| Yang et al. [32] | local | ConDinet++ - Conditional Dilated Convolution Network for Road Extraction from Aerial Images. | | high | ✓Feature Fusion Mechanism ✓Conditional Dilated Convolution Blocks (CDBs) ✓Adaptive Architecture ✓Joint Loss Function ✓Experimental Validation | ✓Complexity ✓Hyperparameter Tuning ✓Training Data Requirement ✓Computation and Resource Requirements ✓Applicability |
| Tan et al. [33] | local | ScaleFusionNet - Enhancing Road Segmentation with Multi-Scale Fusion and Sensitivity | | high | ✓Multi-Scale Fusion ✓End-to-End Architecture ✓Scale Fusion Module ✓Semantic Segmentation Performance ✓Experimental Validation | ✓Computational Complexity ✓Hyperparameter Tuning ✓Training Data Dependence ✓Resource Requirements ✓Model Interpretability ✓Applicability to Other Tasks |
| Zhu et al. [34] | Global | Global Context-aware and Batch-independent Network (GCB-Net) for VHR Satellite Imagery Road Extraction | | high | ✓Global Context Integration ✓Encoder-Decoder Architecture ✓Batch-Independence Enhancemen ✓Multi-Scale Contextual Information ✓Addressing Bias and Transfer Learning ✓Quantitative and Qualitative Performance | ✓Computational Complexity ✓Hyperparameter Tuning ✓Resource Requirements ✓Interpretability Challenges ✓Dataset Generalization ✓Model Complexity vs. Performance Trade-off |
| Wu et al. [35] | local | Dense-Global-Residual Network for Road Extraction from Remote Sensing Images | | high | ✓Spatial Information Preservation ✓Context Awareness Enhancement ✓Performance Improvement ✓Robustness to | ✓Computational Complexity ✓Hyperparameter Tuning ✓Interpretability Challenge ✓Resource Constraints |

Fritz Elenda Nkomba et al.

| Reference | Category | method | Satellite | resolution | Advantages | Disadvantages |
|---|---|---|---|---|---|---|
| | | | | | Occlusions ✓Universal Applicability ✓High-Resolution ZRemote Sensing Imagery | ✓Generalization to Extreme Scenarios ✓Training Data Dependency |
| Zhou et al. [36] | local | Boundary and Topological-aware Road extraction Network (BT-RoadNet) | | high | ✓Boundary and Topological-aware Approach ✓Coarse-to-Fine Architecture ✓Spatial Context Module (SCM) ✓Generalization and Applicability ✓Semantic and Topological Integration | ✓Computational Complexity ✓Hyperparameter Tuning ✓Data Dependency ✓Interpretability Challenge ✓Generalization to Extreme Scenarios ✓Resource Constraints |
| Wu et al. [37] | local | Topology-Based Multi-Task Convolution Network (Bi-HRNet) | | high | ✓Topology-Aware Approach ✓Node Heatmap Learning ✓Bidirectional Connectivity Prediction ✓Non-Maximum Suppression (NMS) ✓Enhanced Accuracy and Completeness ✓State-of-the-Art Performance | ✓Complexity and Resource Demands ✓Hyperparameter Tuning ✓Interpretability Challenges ✓Training Data Requirements |
| Yang et al. [38] | local | CNN-based Road Extraction with Contextual Information | | high | ✓Enhanced Accuracy ✓Incorporation of Contextual Information ✓Foreground Contextual Information (FCI) ✓Position Attention Mechanism ✓Comprehensive Evaluation ✓Semantic and Contextual Features ✓Efficiency | ✓Model Complexity ✓Hyperparameter Tuning ✓Contextual Information Quality ✓Generalization ✓Interpretability ✓Computational Resources |
| Chen et al. [39] | local | Dual-Branch Encoder-Decoder | | high | ✓Enhanced Feature Fusion | ✓Model Complexity |

| Reference | Category | method | Satellite | resolution | Advantages | Disadvantages |
|---|---|---|---|---|---|---|
| | | Road Extraction Network (DBRANet) | | | ✓Effective Feature Extraction ✓Regional Attention Mechanism ✓State-of-the-Art Performance ✓Complex Background Handling ✓Comprehensive Evaluation -Scalability | ✓Hyperparameter Tuning ✓Interpretability ✓Training Data ✓Computational Resources: |
| Dong and Chen [40] | local | Block Multi-Dimensional Attention Network (BMDANet) | | high | ✓Slender Object Handling ✓Cross-Layer Information Exchange ✓Block Multi-Dimensional Attention (BMDA) Module ✓Global Attention Mechanism ✓State-of-the-Art Performance ✓General Applicability ✓Effectiveness Validation | ✓Complexity Considerations ✓Hyperparameter Tuning ✓Training Data ✓Model Interpretability ✓Computational Resources |
| Liu et al. [41] | Hybrid | Residual Attention and Local Context-aware Network (RALC-Net) | | high | ✓Addressing Spatial Heterogeneity ✓Dual-Encoder Structure ✓Residual Attention Module ✓Multi-Scale Dilated Convolution ✓Performance Verification ✓Feature Representation and Generalizability | ✓Complex Architecture ✓Hyperparameter Tuning ✓Dataset Dependency ✓Model Interpretability ✓Resource Requirements ✓Ablation Study Scope |
| Hu et al. [42] | global | WSGAN (Wasserstein GAN) | | high | ✓Multi-Step Approach ✓Clear Outline ✓Salt-and-Pepper Noise Removal ✓Patch GAN | ✓Incomplete Road Network ✓Manual Binary ✓Image Creation ✓Parameter Tuning |

| Reference | Category | method | Satellite | resolution | Advantages | Disadvantages |
|---|---|---|---|---|---|---|
| | | | | | Strategy<br>✓ Weakly Supervised Training:<br>✓ Addressing Shadows | ✓ Training the model requires substantial computational resources<br>✓ Post-Processing Complexity |
| Yang and Wang [43] | local | Ensemble Wasserstein GAN with Gradient Penalty (E-WGAN-GP) | | high | ✓ Highly Challenging Task Addressed<br>✓ Ensemble Strategy<br>✓ Class Imbalance Handling<br>✓ Wasserstein GAN<br>✓ Parameter Optimization<br>✓ Performance Metrics<br>✓ Evaluation on Multiple Datasets | ✓ Complexity and Resource Requirements<br>✓ Model Interpretability<br>✓ Dependency on Training Data<br>✓ Potential Overfitting<br>✓ Ensemble Complexity<br>✓ Generalization to Other Scenarios |
| Abdollahi et al. [44] | local | Deep Learning Approach for Road Extraction from High-Resolution Images with Modified U-Net (MUNet) and Generative Adversarial Neural Network (GAN) | | high | ✓ Use of a Complete Database<br>✓ Use of Data Augmentation Techniques<br>✓ Innovative Network Architecture<br>✓ Use of a GAN Framework | ✓ Limitations in the Recognition of Complex Zones<br>✓ Dependence on Lighting Conditions<br>✓ Road Continuity Problems<br>✓ Computational Complexity<br>✓ Spatial and Spectral Limitations |
| Shamsolmoali et al. [45] | Hybrid | Structured Domain Adaptation with Feature Pyramid Network (SDA-FPN) for Road Extraction | | high | ✓ Addressing Complex Backgrounds<br>✓ Structured Domain Adaptation<br>✓ Incorporation of Feature Pyramid Network<br>✓ Scale-Wise Architecture<br>✓ Joint Reconstruction Loss<br>✓ Superior Performance<br>✓ State-of-the-Art Results | ✓ Domain Adaptation Complexity<br>✓ Data Dependence<br>✓ Hyperparameter Tuning<br>✓ Interpretability<br>✓ Resource Intensity<br>✓ Transferability to Other Scenarios |

| Reference | Category | method | Satellite | resolution | Advantages | Disadvantages |
|---|---|---|---|---|---|---|
| | | | | | ✓ Efficient Parameters | |
| Zhang et al. [46] | Local | Stagewise Domain Adaptation for Road Segmentation (RoadDA) | | high | ✓ Domain Adaptation Focus ✓ Stagewise Approach ✓ Feature Pyramid Fusion ✓ Adversarial Self-Training ✓ Efficient Domain Gap Reduction ✓ State-of-the-Art Performance ✓ Code Availability | ✓ Complexity ✓ Hyperparameter Tuning ✓ Data Dependency ✓ Computational Resources ✓ Interpretability Applicability to Other Domains |
| Wei and Ji [47] | Local | Scribble-Based Weakly Supervised Road Surface Extraction Method (ScRoadExtractor) | | high | ✓ Weakly Supervised Approach ✓ Scribble Label Propagation ✓ Dual-Branch Encoder-Decoder Network ✓ High Performance ✓ Reduced Annotation Effort ✓ Generalizability ✓ Precise Road Surface Segmentation | ✓ Scribble Quality ✓ Dependency on Super-Pixels ✓ Hyperparameter Tuning ✓ Limited to Road Surface Extraction ✓ Computational Resources |
| Ren and al., [48] | Global | Dual-Attention Capsule U-Net (DA-CapsUNet) | | high | ✓ Highly Accurate Road Extraction ✓ Dual-Attention Mechanism ✓ Capsule U-Net Architecture ✓ Multiscale Context-Augmentation ✓ Competitive Performance | ✓ Complex Architecture ✓ Model Interpretability ✓ Resource Intensiveness ✓ Potential Overfitting ✓ Applicability to Unconventional Scenarios |
| Shao and al., [49] | hybrid | RENA - Road Extraction Network with Attention Mechanism | | high | ✓ Utilizing Attention ✓ Characteristic enhancement ✓ Residual Dilated Convolution Module ✓ Improved overall | ✓ Limitation in the face of Missing Information ✓ Dependence on Training Data ✓ Dependence on Training Data ✓ Challenges of Very Dense |

| Reference | Category | method | Satellite | resolution | Advantages | Disadvantages |
|---|---|---|---|---|---|---|
| | | | | | performance<br>✓Adaptability to Vegetation and Missing Information. | Areas |
| Li and al., [50] | Local | Multi-Map Integration Model (MMIM) for Road Extraction from High-Resolution Remote Sensing Images (HRSIs) | | high | ✓Crowdsourced Data Integration<br>✓Noise Robustness Enhancement<br>✓High-Quality Refined Labels<br>✓Avoiding Overfitting<br>✓Smoother and More Complete Results<br>✓Reduced Data Collection Efforts | ✓Data Integration Challenges<br>✓Complex Model<br>✓Label Generation Complexity<br>✓Dependency on Crowdsourced Data<br>✓Generalization to Other Scenarios<br>✓Resource Intensive |
| Lin and al., [51] | Hybrid | United U-Net (UU-Net) for Large-Scale Road Extraction from Optical and SAR Data | | high | ✓Incorporation of Multiple Data Sources<br>✓Improved Accuracy<br>✓Enhanced Generalization<br>✓Spatial Distribution Insights<br>✓Promising Applications<br>✓Multisource Data Synergy | ✓Data Compatibility<br>✓Computational Complexity<br>✓Feature Extraction Challenges<br>✓Data Acquisition and Availability<br>✓Training Data Quantity<br>✓Model Interpretability |
| Zhang and al., [52] | Local | GPS Trajectories-based CNN for Multilevel Urban Road Extraction from High-Resolution Remote Sensing Imagery | | high | ✓Automated Sample Generation<br>✓Efficiency -Multilevel Urban Road Extraction<br>✓CNN Utilization<br>✓Accuracy<br>✓Elimination of Manual Labeling | ✓Data Quality and Availability<br>✓Generalization<br>✓Dependency on GPS Data<br>✓Rasterization and Labeling Challenges<br>✓CNN Complexity<br>✓Trade-off between Accuracy and Data Quality |

## 5.2 Limitations

An approach for the detection of linear structures has been introduced, relying on a combination of wavelet filtering, morphological techniques, and the Watershed algorithm. While this algorithm is effective in highlighting linear structures, there are some limitations associated with this approach. The limitations are as follows:

- Complexity of features: Road networks and urban areas can present a great variability of shapes and textures in images, making it difficult to characterize them accurately using wavelet

filtering and morphological approach techniques. Some linear patterns may be similar to surrounding features, leading to detection confusion.

- Image resolution: The spatial resolution of satellite images or aerial photographs may limit the ability to detect small linear structures or fine details in urban areas. This can lead to a loss of important information and incomplete detection of road networks and urban areas.
- Presence of noise: Satellite images and aerial photographs can be subject to noise and artifact problems, which can alter information and affect the accuracy of linear structure extraction. Noise can lead to detection errors and false alarms.
- Sensitivity to radiometric variations: Radiometric variations in images can be due to differences in lighting conditions, season, vegetation, etc. These variations can complicate the detection of linear structures. These variations can complicate the detection of linear structures, particularly in urban areas where materials and constructions can be very heterogeneous.
- Difficulty with wetlands: Wetlands can have similar visual characteristics to other natural features, making it difficult to distinguish them from satellite or aerial images. Accurate detection of wetlands can be compromised by their complex nature and variability.
- Need for calibration: methods based on wavelet filtering and the morphological approach may require careful calibration of parameters to obtain the best results. This process can be tedious and requires in-depth expertise to achieve optimal results.
- Processing time: Wavelet filtering and the morphological approach can be relatively slow in terms of processing time, particularly for large images or complex scenes. This may limit the applicability of these techniques in real-time or in contexts where rapid analysis is required.

The extraction of road networks and urban fabric (populated areas and wetlands) from satellite images or aerial photographs using wavelet filtering and the morphological approach presents certain limitations and challenges. Although these methods can provide satisfactory results in many cases, it is essential to take these weaknesses into account when interpreting the results and to consider other approaches or combinations of methods to obtain more accurate and complete results.

## 5.3 Implication to society

The detection of linear structures such as road networks, urban areas and wetlands in Cameroon has significant implications for society. Here are some of the main implications:

- Improved urban planning: Accurate detection of urban areas enables authorities to better plan land use, identify areas of urban expansion and make informed decisions on infrastructure and public services.
- Road infrastructure management: Detecting Road networks enables the condition of existing roads to be assessed, areas in need of repair or improvement to be identified, and the construction of new roads to be planned to improve connectivity and facilitate economic development.
- Disaster prevention: Detecting swampy areas can play a vital role in preventing natural disasters such as flooding. By mapping these areas, authorities can better assess potential risks and implement appropriate prevention measures.
- Humanitarian aid and emergency relief: In the event of a natural disaster or emergency, the rapid detection of damaged infrastructures and practicable communication routes facilitates the mobilization of rescue teams and the rapid delivery of humanitarian aid to affected areas.
- Economic development: Accurate mapping of road networks and urban areas promotes economic development by facilitating trade, the movement of goods and people, and stimulating investment in infrastructure.
- Environmental protection: Detecting wetlands helps to preserve the environment by identifying sensitive areas and enabling their conservation or restoration.
- Monitoring environmental change: Regular mapping of linear structures enables us to track changes in the landscape over time, which is essential for monitoring urbanization, the evolution of road networks and environmental change.

The detection of linear structures in Cameroon has cross-cutting implications for society, contributing to urban planning, infrastructure management, disaster prevention, humanitarian aid, economic development, environmental protection, and the monitoring of environmental change. This information provides decision-makers and stakeholders with crucial data to make informed decisions and foster the country's sustainable, resilient development. A complete list of abbreviations is shown in *Appendix I*.

# 6.Conclusion and future work

The extraction of road networks and urban fabric (including populated areas and wetlands) from satellite images or aerial photographs using wavelet filtering and the morphological approach poses significant challenges due to feature complexity, limitations in image resolution, the presence of noise, and sensitivity to radiometric variations. Despite these challenges, the importance of this research has been recognized for infrastructure management, disaster prevention, and the economic and environmental development of Cameroon.

To address these issues and enhance the accuracy of linear structure extraction, future work envisions integrating classification using fuzzy logic, machine learning, or deep learning. These approaches could allow for a more comprehensive characterization of linear structures, considering their radiometric and morphological variability in images. Advanced classification techniques may also aid in distinguishing road networks and urban areas from other surrounding features, thereby improving overall extraction accuracy.

Machine learning, particularly deep learning, can play a crucial role in extracting intricate and subtle information from images by learning patterns from training data. These approaches hold potential for adapting to the specific context of Cameroon, considering local peculiarities and regional variations, for the detection of linear structures.

Future efforts could explore the integration of multi-source data to enhance the robustness of linear structure extraction. Combining satellite, aerial, and terrestrial data may offer a more comprehensive and detailed perspective of road networks and urban areas, contributing to improved decision-making in areas such as land-use planning, infrastructure management, and disaster prevention.

Despite existing limitations, we maintain confidence in the potential of linear structure extraction using wavelet filtering and the morphological approach. We believe that incorporating classification through fuzzy logic, machine learning, or deep learning will open new possibilities for more accurate and efficient applications in the Cameroon context. Subsequent research in this domain will further empower our ability to manage infrastructure, prevent disasters, and foster the sustainable and balanced development of the country.

## References
[1] Gitas IZ, Polychronaki A, Katagis T, Mallinis G. Contribution of remote sensing to disaster management activities: a case study of the large fires in the Peloponnese, Greece. International Journal of Remote Sensing. 2008; 29(6):1847-53.

[2] Rodriguez H, Quarantelli EL, Dynes RR, Thomas DS, Ertugay K, Kemec S. The role of geographic information systems/remote sensing in disaster management. Handbook of Disaster Research. 2007:83-96.

[3] Mohammadzadeh A, Tavakoli A, Valadan ZMJ. Road extraction based on fuzzy logic and mathematical morphology from pan-sharpened IKONOS images. The Photogrammetric Record. 2006; 21(113):44-60.

[4] Chaudhuri D, Kushwaha NK, Samal A. Semi-automated road detection from high resolution satellite images by directional morphological enhancement and segmentation techniques. IEEE Journal of Selected Topics in Applied Earth Observations and Remote Sensing. 2012; 5(5):1538-44.

[5] Jinxin C, Qixin S, Liguang S. A methodology for automatic detection and extraction of road edges from high resolution remote sensing images. In international conference on industrial technology 2006 (pp. 69-74). IEEE.

[6] Sun J, Mao S. River detection algorithm in SAR images based on edge extraction and ridge tracing techniques. International Journal of Remote Sensing. 2011; 32(12):3485-94.

[7] Mena JB, Malpica JA. An automatic method for road extraction in rural and semi-urban areas starting from high resolution satellite imagery. Pattern Recognition Letters. 2005; 26(9):1201-20.

[8] Zhang R, Lin X. Automatic road extraction based on local histogram and support vector data description classifier from very high resolution digital aerial. In international geoscience and remote sensing symposium 2010 (pp. 441-4). IEEE.

[9] Zhu H, Li C, Zhang L, Shen J. River channel extraction from SAR images by combining gray and morphological features. Circuits, Systems, and Signal Processing. 2015; 34:2271-86.

[10] Herumurti D, Uchimura K, Koutaki G, Uemura T. Urban road extraction based on hough transform and region growing. In the 19th korea-japan joint workshop on frontiers of computer vision 2013 (pp. 220-4). IEEE.

[11] Wei QR, Feng DZ. Extracting line features in SAR images through image edge fields. IEEE Geoscience and Remote Sensing Letters. 2016; 13(4):540-4.

[12] Shackelford AK, Davis CH. Urban road network extraction from high-resolution multispectral data. In 2nd GRSS/ISPRS joint workshop on remote sensing

and data fusion over urban areas 2003 (pp. 142-6). IEEE.

[13] Naouai M, Hamouda A, Akkari A, Weber C. New approach for road extraction from high resolution remotely sensed images using the quaternionic wavelet. In pattern recognition and image analysis: 5th Iberian conference, Ib PRIA, las palmas de gran canaria, spain 2011 (pp. 452-9). Springer Berlin Heidelberg.

[14] Begni G, Escafadal R, Fontannaz D, Hong-nga NAT. Remote sensing: a tool for monitoring and assessing desertification, CSFD, 2005; 1-48.

[15] Emran A. Landsat global data on Africa, an example: tracking the spatio-temporal evolution of the city of Rabat in Morocco. In seminars of the United Nations program on space applications. United Nations, New York, 2006 (pp. 15-24). NASA Astrophysics Data System.

[16] Pouyllau M. Remote sensing and the third world Methodologies, practices, new fields and new issues. CNRS editions, Paris; 1991.

[17] Tonyé E, Akono A, Nyoungui AN, Assako RJ. Extraction of the road network on an ERS-2 SAR image and on an HRV (XS) SPOT image by texture analysis and mathematical morphology: application to the city of Yaoundé (Cameroon). Remote sensing in the French-speaking world: critical analysis and perspectives. Ed. AUPELF UREF. 2000:95-103.

[18] Coster M, Chermant JL. Précis d'analyse d'images. Presses du CNRS, Paris; 1989.

[19] Schmitt M, Mattioli J. Morphologie mathématique. Presses des MINES; 2013.

[20] Najman L, Talbot H. Mathematical morphology: from theory to applications. John Wiley & Sons; 2013.

[21] Kombe T, Assako RJ. Mathematical morphology applied to rso images for the differentiation of urban fabrics: case of the city of Douala (Cameroon). Remote Sensing Review. 2007; 7(1-2):3-4.

[22] Nicolas G, Denis L, Tupin F. Detection of line structures in synthetic aperture radar images by generalized likelihood ratio test. In CAP-RFIAP. 2020:1-7.

[23] Tupin F, Gouinaud C, Maitre H, Cretez JP. Detection of the road network on ERS 1 radar images. RFIA AFCET 96 (Rennes). 1996; 43:52.

[24] MaIrte H. A panorama of the hough transform. Signal Processing. 1985; 2(4).

[25] Poncelet N, Cornet Y. Hough transform and lineament detection on satellite images and digital terrain models. Bulletin of the Geographical Society of Liège. 2010; 145-56.

[26] Tupin F, Trouve E, Descombes X, Nicolas JM, Maitre H. Improving IFSAR phase unwrapping by early detection of noninterferometric features. In microwave sensing and synthetic aperture radar 1996 (pp. 250-61). SPIE.

[27] Kombe T, Assato RA. Mathematical morphology applied to SAR images for the detection of urban areas: the case study of the city of Douala. Revue Télédétection. 2007; 7(1-2):3-4.

[28] Lacoste C. Extraction de réseaux linéiques à partir d'images satellitaires et aériennes par processus ponctuels marqués (Doctoral dissertation, Université Nice Sophia Antipolis). 2004.

[29] Zhang X, Ma W, Li C, Wu J, Tang X, Jiao L. Fully convolutional network-based ensemble method for road extraction from aerial images. IEEE Geoscience and Remote Sensing Letters. 2019; 17(10):1777-81.

[30] Li P, He X, Qiao M, Cheng X, Li Z, Luo H, et al. Robust deep neural networks for road extraction from remote sensing images. IEEE Transactions on Geoscience and Remote Sensing. 2020; 59(7):6182-97.

[31] Li P, He X, Qiao M, Cheng X, Li J, Guo X, et al. Exploring label probability sequence to robustly learn deep convolutional neural networks for road extraction with noisy datasets. IEEE Transactions on Geoscience and Remote Sensing. 2021; 60:1-8.

[32] Yang K, Yi J, Chen A, Liu J, Chen W. ConDinet++: full-scale fusion network based on conditional dilated convolution to extract roads from remote sensing images. IEEE Geoscience and Remote Sensing Letters. 2021; 19:1-5.

[33] Tan X, Xiao Z, Wan Q, Shao W. Scale sensitive neural network for road segmentation in high-resolution remote sensing images. IEEE Geoscience and Remote Sensing Letters. 2020; 18(3):533-7.

[34] Zhu Q, Zhang Y, Wang L, Zhong Y, Guan Q, Lu X, et al. A global context-aware and batch-independent network for road extraction from VHR satellite imagery. ISPRS Journal of Photogrammetry and Remote Sensing. 2021; 175:353-65.

[35] Wu Q, Luo F, Wu P, Wang B, Yang H, Wu Y. Automatic road extraction from high-resolution remote sensing images using a method based on densely connected spatial feature-enhanced pyramid. IEEE Journal of Selected Topics in Applied Earth Observations and Remote Sensing. 2020; 14:3-17.

[36] Zhou M, Sui H, Chen S, Wang J, Chen X. BT-RoadNet: a boundary and topologically-aware neural network for road extraction from high-resolution remote sensing imagery. ISPRS Journal of Photogrammetry and Remote Sensing. 2020; 168:288-306.

[37] Wu Z, Zhang J, Zhang L, Liu X, Qiao H. Bi-HRNet: a road extraction framework from satellite imagery based on node heatmap and bidirectional connectivity. Remote Sensing. 2022; 14(7):1732.

[38] Yang Z, Zhou D, Yang Y, Zhang J, Chen Z. TransRoadNet: a novel road extraction method for remote sensing images via combining high-level semantic feature and context. IEEE Geoscience and Remote Sensing Letters. 2022; 19:1-5.

[39] Chen SB, Ji YX, Tang J, Luo B, Wang WQ, Lv K. DBRANet: road extraction by dual-branch encoder and regional attention decoder. IEEE Geoscience and Remote Sensing Letters. 2021; 19:1-5.

[40] Dong S, Chen Z. Block multi-dimensional attention for road segmentation in remote sensing imagery.

Fritz Elenda Nkomba et al.

IEEE Geoscience and Remote Sensing Letters. 2021; 19:1-5.

[41] Liu Z, Wang M, Wang F, Ji X. A residual attention and local context-aware network for road extraction from high-resolution remote sensing imagery. Remote Sensing. 2021; 13(24):1-20.

[42] Hu A, Chen S, Wu L, Xie Z, Qiu Q, Xu Y. WSGAN: an improved generative adversarial network for remote sensing image road network extraction by weakly supervised processing. Remote Sensing. 2021; 13(13):1-18.

[43] Yang C, Wang Z. An ensemble Wasserstein generative adversarial network method for road extraction from high resolution remote sensing images in rural areas. IEEE Access. 2020; 8:174317-24.

[44] Abdollahi A, Pradhan B, Sharma G, Maulud KN, Alamri A. Improving road semantic segmentation using generative adversarial network. IEEE Access. 2021; 9:64381-92.

[45] Shamsolmoali P, Zareapoor M, Zhou H, Wang R, Yang J. Road segmentation for remote sensing images using adversarial spatial pyramid networks. IEEE Transactions on Geoscience and Remote Sensing. 2020; 59(6):4673-88.

[46] Zhang L, Lan M, Zhang J, Tao D. Stagewise unsupervised domain adaptation with adversarial self-training for road segmentation of remote-sensing images. IEEE Transactions on Geoscience and Remote Sensing. 2021; 60:1-3.

[47] Wei Y, Ji S. Scribble-based weakly supervised deep learning for road surface extraction from remote sensing images. IEEE Transactions on Geoscience and Remote Sensing. 2021; 60:1-2.

[48] Ren Y, Yu Y, Guan H. DA-CapsUNet: a dual-attention capsule U-Net for road extraction from remote sensing imagery. Remote Sensing. 2020; 12(18):1-17.

[49] Shao S, Xiao L, Lin L, Ren C, Tian J. Road extraction convolutional neural network with embedded attention mechanism for remote sensing imagery. Remote Sensing. 2022; 14(9):1-18.

[50] Li P, He X, Qiao M, Miao D, Cheng X, Song D, et al. Exploring multiple crowdsourced data to learn deep convolutional neural networks for road extraction. International Journal of Applied Earth Observation and Geoinformation. 2021; 104:102544.

[51] Lin Y, Wan L, Zhang H, Wei S, Ma P, Li Y, et al. Leveraging optical and SAR data with a UU-Net for large-scale road extraction. International Journal of Applied Earth Observation and Geoinformation. 2021; 103:102498.

[52] Zhang J, Hu Q, Li J, Ai M. Learning from GPS trajectories of floating car for CNN-based urban road extraction with high-resolution satellite imagery. IEEE Transactions on Geoscience and Remote Sensing. 2020; 59(3):1836-47.

[53] Girard MC, Girard CM. Télédétection appliquée. Zones tempérées intertropicales [Applied remote sensing in intertropical temperate zones]. Partie pédologie. 1989:192-233.

[54] Wang L. Un nouvel espace de texture. International Journal of Remote Sensing. 1994; 15(8):1713-23.

[55] Cocquerez JP, Philipp S, Bolon P, Chassery JM, Demigny D, Graffigne C, et al. Analyse d'images: filtrage et segmentation. Masson; 1995.

[56] Vincent L, Soille P. Watersheds in digital spaces: an efficient algorithm based on immersion simulations. IEEE Transactions on Pattern Analysis & Machine Intelligence. 1991; 13(06):583-98.

[57] Zheng C, Yao H. Segmentation for remote-sensing imagery using the object-based Gaussian-Markov random field model with region coefficients. International Journal of Remote Sensing. 2019; 40(11):4441-72.

[58] https://theses-algerie.com/2803423358558140/memoire-de-magister/universite-abou-bekr-belkaid---tlemcen/extraction-de-r%C3%A9seaux-lin%C3%A9iques-%C3%A0-partir-des-images-%C3%A0-hauter%C3%A9solution. Accessed 10 July 2023.

[59] Risson V. Application de la morphologie mathématique à l'analyse des conditions d'éclairage des images couleur (Doctoral dissertation, École Nationale Supérieure des Mines de Paris). 2001.

[60] Beucher S. Segmentation d'images et morphologie mathématique (Doctoral dissertation, Ecole Nationale Supérieure des Mines de Paris). 1990.

[61] Attia D. Segmentation d'images par combinaison adaptative couleur-texture et classification de pixels.: applications à la caractérisation de l'environnement de réception de signaux GNSS (Doctoral dissertation, Université de Technologie de Belfort-Montbeliard). 2013.

[62] Strauss O, Comby F. Fuzzy morphological operations with variable kernels for omnidirectional single-viewpoint images. Signal Processing. 2005; 22(5):1-23.

**Elenda Nkomba Fritz** is an Assistant Professor in the Computer Science and Engineering department at the University of Douala, Cameroon. He earned his Bachelor of Engineering (B.E.) and M.Tech degrees in Mathematics, Computer Science, Artificial Intelligence, and Electrical Engineering. His research interests encompass a diverse range, including Image Processing, Data Mining, Optimization, Machine Learning, Cloud Computing, Data Science, and Artificial Intelligence.
Email: elendankombafritz@gmail.com
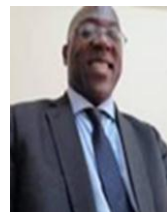
**Kombe Timothée** holds a Doctor of Philosophy degree from the University of Douala, Cameroon, with a specialization in Mechanical Engineering, Image Processing, and Control Systems Engineering. His extensive skills and expertise cover a wide array of disciplines, including

Hybrid Automatic Systems, Materials Modelization, Electrical Power Engineering, Power Electronics, Power Converters, Inverters, Power Microgrids, Optimization, Maintenance of Electrical and Machinery Equipment, Electrical and Electronics Engineering, Transformers, Power System Stability, Voltage Regulation, and Electrical Protection.
Email: tkombe@yahoo.fr

**Ele Pierre** holds a Doctor of Philosophy degree from the University of Yaoundé I, Cameroon. His skills and expertise encompass a variety of areas, including Neuro-Fuzzy systems, data compression, image processing, compression techniques, simulation in Electrical & Electronics Engineering, Renewable Energy Technologies, Power Electronics, Power Systems Modelling, and Harmonics Activity.
Email: pierre_ele@yahoo.fr

**Appendix I**

| S. No. | Abbreviation | Description |
|---|---|---|
| 1 | CNN | Convolutional Neural Network |
| 2 | DNNs | Deep Neural Networks |
| 3 | EPL | Extended Predicate Logic |
| 4 | ERS | European Remote Sensing Satellite |
| 5 | ESA | European Space Agency |
| 6 | FCN | Fully Convolutional Network |
| 7 | GAN | Generative Adversarial Neural Network |
| 8 | HRSIs | High-Resolution Remote Sensing Images |
| 9 | IT | Information Technology |
| 10 | MRA | Multiresolution Analysis |
| 11 | RALC-Net | Residual Attention and Local Context-aware Network |
| 12 | SAR | Synthetic Aperture Radar |
| 13 | SDA-FPN | Structured Domain Adaptation with Feature Pyramid Network |
| 14 | WSGAN | Wasserstein Generative Adversarial Network |